Author Manuscript

Author Manuscript

Author Manuscript

Author Manuscript

HHS Public Access

Author manuscript

*Nat Metab*. Author manuscript; available in PMC 2020 December 16.

Published in final edited form as:

*Nat Metab*. 2020 June ; 2(6): 547–557. doi:10.1038/s42255-020-0213-x.

# *In vivo* studies of glucagon secretion by human islets transplanted in mice

**Krissie Tellez**[1,6], **Yan Hang**[1,2,6], **Xueying Gu**[1], **Charles A. Chang**[1], **Roland W. Stein**[3,4], **Seung K. Kim**[1,2,5]

[1]Department of Developmental Biology, Stanford University School of Medicine, Stanford, CA, USA

[2]Stanford Diabetes Research Center, Stanford University School of Medicine, Stanford, CA, USA

[3]Department of Molecular Physiology and Biophysics, Vanderbilt University Medical Center, Nashville TN, USA

[4]Department of Cell and Developmental Biology, Vanderbilt University Medical Center, Nashville TN, USA

[5]Department of Medicine (Endocrinology Division), Stanford University School of Medicine, Stanford, CA, USA

[6]These authors contributed equally.

## Abstract

Little is known about regulated glucagon secretion by human islet α cells compared to insulin secretion from β cells, despite conclusive evidence of dysfunction in both cell types in diabetes mellitus. Distinct insulins in humans and mice permit *in vivo* studies of human β cell regulation after human islet transplantation in immunocompromised mice, whereas identical glucagon sequences prevent analogous *in vivo* measures of glucagon output from human α cells. Here we use CRISPR/Cas9 editing to remove glucagon codons 2–29 in immunocompromised *NSG* mice, preserving production of other proglucagon-derived hormones. *Glucagon knockout-NSG* (*GKO-NSG*) mice have metabolic, liver and pancreatic phenotypes associated with glucagon signaling deficits that revert after transplantation of human islets from non-diabetic donors. Glucagon hypersecretion by transplanted islets from donors with type 2 diabetes revealed islet-intrinsic

Users may view, print, copy, and download text and data-mine the content in such documents, for the purposes of academic research, subject always to the full Conditions of use:http://www.nature.com/authors/editorial_policies/license.html#terms

Communicating author: Seung K. Kim, M.D., Ph.D., 279 Campus Drive, Stanford, CA 94305, Telephone: (650) 723-6230, Fax: (659) 725-7739, seungkim@stanford.edu.

Author Contributions

Conceptualization: S.K.K., K.T. and Y.H.; Methodology: K.T. and Y.H., and S.K.K. Validation: K.T., Y.H., and X.G; Formal Analysis: K.T. and X.G.; Investigation: K.T., Y.H., X.G., and C.A.C.; Data Curation: K.T.; Writing - Original Draft: K.T. and S.K.K.; Writing - Review and Editing: K.T., Y.H., R.W.S., and S.K.K.; Visualization: K.T. and Y.H.; Supervision: R.W.S. and S.K.K; Project Administration: S.K.K.; Funding Acquisition: S.K.K.

Data Availability

The data that support the findings of this study are available from the corresponding author upon request.

Declaration of Interests

The authors declare no competing interests.

Author Manuscript Author Manuscript Author Manuscript Author Manuscript

defects. We suggest that *GKO-NSG* mice provide an unprecedented resource to investigate human α cell regulation *in vivo*.

**Keywords**

diabetes mellitus; insulin; hormone; liver; pancreas; Slc38a5; GLP-1; incretin; proglucagon; genetics; disease

Pancreatic islet α and β cells play an important role in maintaining euglycemia by secreting peptide hormones in response to glucose and other blood metabolites. In healthy β cells, an increase in blood glucose triggers insulin secretion, which promotes glucose uptake and glycogenesis or adipogenesis in 'insulin-target' organs. In contrast, α cell glucagon secretion, stimulated by hypoglycemia, amino acids, adrenal and neuronal inputs, leads to glucose mobilization by promoting glycogenolysis and gluconeogenesis in 'glucagon-target' organs, like liver[1]. Impaired regulation or output of insulin and glucagon by human β cells and α cells underlies development and progression of diabetes mellitus. Thus, intensive efforts are focused on determining the physiological and pathological mechanisms governing human islet α cell and β cell function.

Recent studies reveal that human and mouse islet cells have differences in cellular composition, molecular regulation, physiological control, intra-islet cell interactions and other crucial properties[2–5], motivating increased research focus and resource generation in human islet biology. Transplantation of human islets in immunocompromised mice, like the *NOD.Cg-Prkdc*$^{scid}$*Il2rg*$^{tm1Wjl}$*Sz* mice (*NSG*) strain[6,7], has emerged as an important strategy for assessing human islet β cell function *in vivo*[8–10]. Unlike distinct human and mouse insulins, the mature glucagon sequence in these species is identical, precluding accurate quantification of circulating human islet-derived glucagon secretion in mice and limiting studies of human α cells in transplantation-based models. Thus, development of immunocompromised mouse strains that permit detection of human glucagon in mice and *in vivo* studies of transplanted human islet α cell function could be transformative by enabling mechanistic analysis in physiological and pathophysiological conditions.

Genetic targeting to eliminate endogenous glucagon production in mice could permit *in vivo* quantification of glucagon output by transplanted human islets. The *Gcg* gene encodes proglucagon, a prohormone expressed and differentially processed in islet α cells, gut enteroendocrine cells, and the central nervous system to produce multiple distinct peptide hormone products, including glucagon, oxyntomodulin, glicentin, glucagon-like peptide-1 (GLP-1) and glucagon-like peptide 2 (GLP-2)[11]. Differential proglucagon processing depends on co-expression of the prohormone convertase (PC) enzymes. In pancreatic islet α cells, PC2 enables cleavage of proglucagon into the 29 amino acid mature glucagon protein, which is entirely encoded[12] by *Gcg* exon 3. PC1/3 expression in enteroendocrine cells permits cleavage of proglucagon into other products, including GLP-1, a secreted incretin hormone that enhances postprandial insulin output by islet β cells[13–17].

Glucagon production in mice has been eliminated by targeted mutation of the *Gcg* gene to generate the *Gcg*$^{gfp}$ allele; adult homozygous *Gcg*$^{gfp/gfp}$ mice were normoglycemic and

Author Manuscript Author Manuscript Author Manuscript Author Manuscript

exhibited α cell hyperplasia and hypoinsulinemia[18]. Earlier studies in mice of glucagon signaling loss from glucagon receptor (*Gcgr*) deletion, Gcgr antibody inactivation[19–22], or elimination of PC2[23, 24] reported extensive metabolic phenotypes reflecting impaired gluconeogenesis and glycogenolysis, including elevated circulating amino acid levels and basal hypoglycemia. Despite this progress, none of the mice from these prior studies afforded the possibility of investigating glucagon regulation by transplanted human islet α cells. Here we generated immunocompromised mice lacking mature glucagon coding sequences (*GKO-NSG*) that enable investigations of glucagon regulation in transplanted human islets. We demonstrate the utility of *GKO-NSG* mice for analyzing *in vivo* α cell function in human islets from non-diabetic and diabetic donors.

## Results

### Generation of GKO-NSG mice

To develop mice that permit transplantation of human islets and detection of human glucagon, we used CRISPR/Cas9 genome editing in *NSG*-derived oocytes to create an in-frame deletion of nucleotides from *Gcg* exon 3, which encode mature glucagon (Figure 1a **and** Extended Data 1a). This strategy should preserve production of metabolic regulators derived from the proglucagon carboxy-terminus, including GLP-1. After generating candidate founder mice, genotype screening identified one *NSG* founder harboring an in-frame 93 base pair (bp) deletion of the 3' end of *Gcg* exon 3. This in-frame deletion includes the elimination of 84 nucleotides encoding amino acids 2–29 of mature glucagon (Figures 1a-b **and** Extended Data 1a). Subsequent breeding of heterozygous F1 mice produced viable, fertile homozygous *GKO-NSG* mice that were born at a rate of 22.1% (compared to 32.8% wild type, and 45.1% heterozygous; n= 122 mice). Three-week-old male and female *GKO-NSG* mice weighed significantly less than *NSG* control littermates (Extended Data 1c). However, by eight weeks of age, no difference in body weight was detected in adult *NSG* and *GKO-NSG* mice (Extended Data 1c). This transient reduction of body mass in *GKO-NSG* mice likely reflects a combination of reduced circulating insulin levels in *GKO-NSG* mice (see below), and possibly unrecognized roles for glucagon in development[25–28]. Thus, beginning at eight weeks of age, *GKO-NSG* mice of both sexes were characterized for phenotypes associated with glucagon signaling loss.

To verify elimination of mature glucagon production in *GKO-NSG* mice, plasma glucagon levels were measured from *ad libitum* fed and fasted *GKO-NSG* and *NSG* control mice. Unlike control *NSG* mice, plasma glucagon was undetectable in *GKO-NSG* mice in both fed and fasted states (Figure 1c). Consistent with this, immunostaining with antibodies that detect mature glucagon (GCG 1–29) did not label islet α cells in *GKO-NSG* pancreata, whereas these α cells were readily identified with an antibody that detects proglucagon (Extended Data 1b). By contrast, plasma total and active GLP-1 levels following an oral glucose tolerance test were higher in *GKO-NSG* mice compared to *NSG* control littermates (Figure 1d **and** Extended Data 1f). Similar to previous studies using glucagon-signaling deficient mice[19, 29], extracts of isolated islets from *GKO-NSG* mice had increased active GLP-1 levels that may account for increased circulating GLP-1 (Extended Data 1g). This increase in circulating GLP-1 was accompanied by lower glycemic levels in both fasting and

Author Manuscript Author Manuscript Author Manuscript Author Manuscript

feeding (Extended Data 1d), as well as improved glucose tolerance (Extended Data 1e) in *GKO-NSG* mice. Thus, our CRISPR-based strategy successfully eliminated glucagon while sparing GLP-1 production in *GKO-NSG* mice.

## Transplanted human islets retain regulated glucagon secretion in GKO-NSG mice

To assess the possibility of measuring circulating glucagon from human islets in *GKO-NSG* mice, we transplanted human islets from previously-healthy donors under the renal capsule of *GKO-NSG* mice (*GKO-NSG* Tx mice; Figure 2a). Plasma glucagon was detectable in *GKO-NSG* Tx mice two weeks after transplantation and thereafter for at least fourteen weeks, at which point *GKO-NSG* Tx mice were sacrificed for tissue analysis. Four weeks after human islet transplantation, plasma glucagon levels in fasted *GKO-NSG* Tx and control *NSG* mice were remarkably similar, but circulating glucagon remained undetectable in sham-transplanted *GKO-NSG* mice (Figure 2b).

To assess dynamic regulation of glucagon secretion from human α cells in *GKO-NSG* Tx mice, we measured glucagon secretion *in vivo* after an intraperitoneal insulin challenge, which elicits transient hypoglycemia. Reduced blood glucose levels stimulate α cell glucagon secretion[1, 30], and, as expected, acute hypoglycemia was accompanied by increased circulating glucagon levels in *NSG* controls (Figures 2c **and** Extended Data 2). By contrast, insulin challenge and hypoglycemia elicited no glucagon output in sham-transplanted *GKO-NSG* mice (Figure 2c **and** Extended Data 2). Like in *NSG* controls, circulating human islet-derived glucagon levels increased upon induction of hypoglycemia in *GKO-NSG* Tx mice (Figure 2c **and** Extended Data 2). As transplanted human islets are the sole source of circulating glucagon in *GKO-NSG* Tx mice, we conclude that insulin challenge and ensuing transient hypoglycemia evoked glucagon secretion by human α cells in these mice, an *in vivo* response not previously reported for human islets transplanted in mice. These results suggest human α cell mechanisms governing regulated glucagon secretion remained intact after transplantation.

## Human islets establish a glucagon-signaling axis that corrects liver phenotypes in GKO-NSG mice

Glucagon signaling is an essential regulator of hepatic amino acid metabolism, gluconeogenesis, and glycogenolysis[20, 31, 32]. Consistent with prior mouse models of impaired glucagon signaling from glucagon or glucagon receptor deficiency[20–22], we observed increased total plasma amino acid levels in *GKO-NSG* mice compared to *NSG* control littermates (Figure 3a). Moreover, measures of individual amino acids from plasma revealed that 23 of 28 amino acids profiled were significantly increased in *GKO-NSG* mice (Figure 3b **and** Extended Data 3). To examine if these changes could result from altered hepatic metabolism, expression of genes encoding enzymes involved in gluconeogenesis (*G6pc and Pepck)* and amino acid metabolism (*Tat*, *Oat, Nnmt,* and *Gls2*) were measured by qPCR. *G6pc*, *Tat*, *Oat* and *Gls2* were significantly decreased in *GKO-NSG* mice compared to *NSG* controls (Figure 3d). To assess differences in glycogenolysis, liver glycogen levels were measured from fasted *GKO-NSG* and *NSG* control mice. We observed a trend of increased average hepatic glycogen levels in *GKO-NSG* mice compared to *NSG* controls (Figure 3c). Together, these data suggest that, like in previous studies of glucagon signaling

Author Manuscript Author Manuscript Author Manuscript Author Manuscript

loss[20–22, 24, 33], gluconeogenesis and amino acid metabolism are impaired in *GKO-NSG* mice.

To determine if human islet-derived glucagon was able to rescue the phenotypes found in *GKO-NSG* host tissues, we examined *GKO-NSG* Tx mice fourteen weeks after human islet transplantation. The liver defects were corrected, including reduction of total and individual plasma amino acids (Figures 3a-b **and** Extended Data 3), decreased liver glycogen levels (Figure 3c), and normalization of hepatic *G6pc, Tat, Oat,* and *Gls2* expression (Figure 3d). Together, these findings suggest that glucagon secretion by human islet grafts durably reconstituted a physiological islet-liver signaling axis in *GKO-NSG* mice.

## Glucagon secreted by human islet grafts corrects α cell hyperplasia in GKO-NSG mice

Impaired glucagon signaling in mice can evoke compensatory α cell proliferation and hyperplasia[19, 23, 24, 34]. Elevated circulating amino acids in mice lacking glucagon signaling were previously demonstrated to induce α cell proliferation and hyperplasia[20–22] through a mechanism involving an amino acid transporter, Slc38a5 [20, 21]. As *GKO-NSG* mice exhibited hyperaminoacidemia, we assessed islet α cell and β cell hyperplasia and proliferation in *GKO-NSG* islets. For α cell morphometry in *GKO-NSG* islets, we used a proglucagon-specific antibody that detected both wild type and internally-deleted GKO proglucagon (proglucagonΔ). Antibodies to MafB, an adult α cell-specific islet transcription factor in mice[35] (Figures 4a-c), were also used to identify changes in islet α cell mass. Islet morphometry in adult *GKO-NSG* mice revealed an increased percentage of α cells expressing the proliferation marker Ki67 (Figures 4e-h) and increased α cell mass (Figures 4a-d). No differences were observed in β cell mass or proliferation in islets of *GKO-NSG* and *NSG* control mice (Figures 4a-h). To examine if α cell hyperplasia might be driven by a previously described mechanism involving *Slc38a5* [20, 21], islets from *GKO-NSG* and *NSG* control mice were surveyed for Slc38a5 protein production. As expected, *GKO-NSG* mice showed increased α cell production of Slc38a5 compared to islets from *NSG* control mice and, as previously reported[36], we also detected Slc38a5 in acinar cells (Figures 4i-n). Thus, like in prior models of glucagon deficiency, we observed adaptive α cell expansion, stimulated by hyperaminoacidemia and accompanied by increased α cell Slc38a5 production.

Since human glucagon from islet grafts restored circulating amino acid levels in *GKO-NSG* mice (Figures 3a-b), we next assessed the impact on host islet α cells in *GKO-NSG* Tx mice and controls. Morphometry analysis revealed that host α cell mass ‘normalized’ in *GKO-NSG* Tx mice compared to *NSG* control mouse islets (Figures 4c-d), and was accompanied by a reduction in the number of proglucagon$\Delta^+$ Ki67$^+$ cells (Figures 4g-h), and loss of Slc38a5 in mouse α cells (Figures 4o-q). Thus, restoration of glucagon signaling by human islet grafts in *GKO-NSG* mice corrected adaptive pancreatic islet α cell expansion observed in *GKO-NSG* mice. However, further studies are needed to assess the basis of this correction, including the possibility of α cell apoptosis[24].

Author Manuscript Author Manuscript Author Manuscript Author Manuscript

## Restoration of glucose and insulin regulation in transplanted GKO-NSG mice

Glucagon increases blood glucose levels by promoting hepatic glucose output, and is also implicated in regulating normal insulin secretion[37–39]. Hence, mice lacking glucagon signaling are hypoinsulinemic[18] and hypoglycemic[19, 23, 33]. Consistent with these extant glucagon signaling mutant mouse models, *GKO-NSG* mice had chronically reduced blood glucose levels and lower *ad libitum* fed plasma insulin levels compared to *NSG* control mice (Figures 5a-b, Extended Data 1d, **and** Extended Data 4b-c). Four weeks after human islet transplantation, *ad libitum* fed blood glucose and total plasma insulin levels in *GKO-NSG* Tx mice were increased and indistinguishable from *NSG* controls (Figures 5a-b **and** Extended Data 4b-c). In *GKO-NSG* Tx mice, total plasma insulin levels reflected contributions from both host mouse β cells and transplanted human islets (Figure 5b **and** Extended Data 4d). While circulating glucagon levels differed in *ad libitum* fed *NSG* and *GKO-NSG* Tx mice, human glucagon in *GKO-NSG* Tx mice was sufficient to maintain normoglycemia (Figures 2b, 5a, **and** Extended Data 4a-b). Thus, transplanted human islets improved glycemic and insulin control in *GKO-NSG* Tx mice.

To examine insulin and glucose regulation further in *GKO-NSG* mice after human islet transplantation, we performed an intraperitoneal glucose challenge. Compared to *NSG* controls, glucose clearance by *GKO-NSG* mice was faster (Figure 5c) and accompanied by an exaggerated (mouse) insulin excursion (Figure 5d). Glucose and insulin excursions in *GKO-NSG* Tx mice more closely resembled that of *NSG* controls (Figures 5c-d). Dynamic total circulating insulin levels in *GKO-NSG* Tx mice reflected a combination of mouse and human insulins (Figures 5d-e). Notably, it appeared that human insulin release from transplanted islets was well-regulated during glucose challenge, including an acute hormone rise followed by clearance from the circulation (Figure 5e). These data suggest that human islet-derived glucagon improved glycemic and insulin regulation in *GKO-NSG* Tx mice, and thus highlight the role of glucagon in maintaining euglycemia and normal insulin secretion.

## Excessive glucagon secretion by transplanted T2D islets in GKO-NSG mice

Type 2 diabetes mellitus is often associated with increased circulating glucagon levels, which appear less responsive to inhibitory elevations in blood glucose[40, 41]. However, it remains unclear if hyperglucagonemia in T2D reflects increased glucagon secretion by islets. We used *in vitro* assays and human islet transplantation into *GKO-NSG* mice to examine glucagon secretion by islets from subjects with T2D (Extended Data 5 and Figure 6). Compared to control islets from non-diabetic donors, islets from T2D donors had similar increases of glucagon secretion in response to glucose reduction *in vitro*: however, in 2 out of 3 T2D donor islets, the response to the secretagogue L-arginine was exaggerated (Extended Data 5a). Transplantation of T2D islets into *GKO-NSG* mice (hereafter, *GKO-NSG* Tx T2D) led to elevated plasma glucagon levels (Figure 6b **and** Extended Data 5c). However, there was no detectable difference in islet glucagon content between non-diabetic and T2D donors (Extended Data 5b). Hyperglucagonemia was accompanied by an average glycemic increase of 32 mg/dL in fasted *GKO-NSG* Tx T2D mice, (96± 8 vs. 128 ± 8 mg/dL; $P = 0.042886$; Extended Data 5d), and a trend toward increased glycemia during *ad libitum* feeding ($P = 0.071059$; Figure 6a).

Author Manuscript Author Manuscript Author Manuscript Author Manuscript

Despite relative hyperglycemia and hyperglucagonemia in *GKO-NSG* Tx T2D mice, circulating total and human islet-derived insulin levels in these mice were comparable to those in *GKO-NSG* mice transplanted with islets from non-diabetic donors (Figures 6c-d **and** Extended Data 5e). When challenged with insulin and subsequent transient hypoglycemia, *GKO-NSG* Tx T2D mice had elevated plasma glucagon levels compared to *GKO-NSG* mice transplanted with non-diabetic human islets (Figure 6e and Extended Data 5f). Collectively, these results demonstrate that hyperglucagonemia in T2D reflects intrinsic islet defects in regulated glucagon secretion. Moreover, compared to *in vitro* secretion studies, defective T2D islet secretion was more robustly detected after transplantation in *GKO-NSG* mice, highlighting the need for *in vivo* systems to assess glucagon secretion.

## Discussion

To address the absence of animal models to study regulated glucagon secretion from human islet α cells *in vivo*, here we used CRISPR/Cas9 to develop the *GKO-NSG* mouse. Human islets engrafted durably in *GKO-NSG* mice and retained regulated glucagon and insulin secretion. Reconstituting glucagon signaling to 'glucagon-target' organs like the pancreas and liver rescued multiple phenotypes associated with glucagon deficiency, including deviations in circulating glucose, amino acid, and insulin levels. Additionally, we provide index evidence that transplanted islets from human donors with T2D display chronically elevated glucagon output, accompanied by significantly increased blood glucose levels. Prior reports of mice that lack glucagon signaling[18–23, 29, 42] revealed many phenotypes associated with loss of glucagon signaling in pancreatic islets and other organs - phenotypes that we observed in *GKO-NSG* mice. However, *GKO-NSG* mice also have distinct properties not previously reported[18, 23, 29], likely reflecting preserved production of 'nested' proglucagon-derived peptides like GRPP, GLP-1, and GLP-2, in addition to the superior receptivity of the *NSG* strain background to xenotransplantation[6, 7]. While our approach led to the unavoidable loss of the oxyntomodulin and glicentin peptide hormones (which incorporate amino acids 1–29 of GCG), this also creates opportunities to study the *in vivo* functions of these hormones in *GKO-NSG* mice.

Glucagon is a crucial intercellular and inter-organ regulator of pancreatic islet cells, liver, and other organs[43]. Our results suggest that the *GKO-NSG* model should be useful for investigating these signaling interactions. Here, we observed that hyperaminoacidemia, hypoglycemia, α cell hyperplasia, and islet Slc38a5 production in *GKO-NSG* mice are reversed after human islet transplantation, indicating (re)-establishment of at least two homeostatic *in vivo* signaling axes mediated by human glucagon and circulating amino acids. The first signaling axis links transplanted human islets to the host liver and the second links the liver to native pancreatic islets cells. Reversion of hyperaminoacidemia and hypoglycemia reflect signaling of human glucagon to the host *GKO-NSG* liver, which then appropriately triggers glycogenolysis, gluconeogenesis, and amino acid metabolism to correct hypoglycemia (Figures 3 **and** 5a). Thus, *GKO-NSG* mice should be useful in future studies to determine how α cells regulate glycemic levels, a phenotype that likely reflects multiple signals between the host liver and islets. For example, systematic modulation of variables like the number of transplanted human islets[44] in *GKO-NSG* mice could be used to clarify the basis of distinct[44, 45] mouse and human glycemic 'set-points'. While reversion of

Author Manuscript Author Manuscript Author Manuscript Author Manuscript

liver phenotypes is largely driven by human islet-derived glucagon signaling, reversion of α cell hyperplasia in *GKO-NSG* Tx mice likely reflects corrected liver to native pancreas signaling. However, further studies are needed to assess the basis for this observation, including the possibility of host α cell apoptosis with glucagon repletion [24].

Studies here also demonstrate powerful ways the *GKO-NSG* mouse can be used to investigate human islets from subjects with diseases like diabetes. For example, our work compared *in vivo* glucagon output by transplanted islets from non-diabetic and T2D donors, and revealed that T2D islets maintained significantly increased glucagon output, providing index *in vivo* evidence that islet-intrinsic or α cell-intrinsic defects lead to excessive glucagon secretion in T2D. Moreover, relative hyperglucagonemia in *GKO-NSG* mice transplanted with T2D human islets was accompanied by a significant increase in fasted blood glucose levels, compared to mice transplanted with islets from non-diabetic donors. These data suggest that glucagon hypersecretion by islets in T2D may contribute to hyperglycemia. Notably, human insulin output in *GKO-NSG* Tx T2D mice did not increase in response to the elevated glycemic levels, indicating that β cell dysfunction is also maintained after T2D islet transplantation in *GKO-NSG* mice.

To evaluate the function of candidate T2D risk genes identified by GWAS and discover human islet β cell regulators, we previously used loss-, and gain-of-function genetics in human pseudo-islets transplanted in *NSG* mice[4, 10]. This experimental logic, using *GKO-NSG* mice, can be expanded to human α cells in islets from previously-healthy, pre-diabetic, or diabetic donors. Thus, we can now examine how α cell enriched genes[3, 46] and genetic changes in diabetes mellitus[3, 47, 48] impact human α cell identity and function. Aside from intrinsic genetic mechanisms governing hormone secretion from islet cells, intra-islet signaling between α cells, β cells, δ cells, and other islet cells is also known to regulate islet hormone secretion[1, 37, 38, 49–55]. To the extent that regulated interactions between human α cells, β cells, and δ cells are reconstituted and measurable in *GKO-NSG* mice, these mice could be useful for *in vivo* studies of these and other intra-islet signaling interactions. Moreover, we envision that *GKO-NSG* mice transplanted with islets from human donors (or other species) will be useful for examining how pharmacological agents, or acquired environmental stressors, like starvation or diet-induced obesity, impact human α cells. Using *NSG* mice, we recently reported that responses of transplanted human islet β cells to high fat diet challenge were distinct from those observed in (host) mouse β cells[9]. Additionally, *GKO-NSG* mice should be useful for assessing the function of transplanted islet-like cells produced from renewable sources like human stem cell lines[56–60]. Thus, *GKO-NSG* mice should be a valuable resource for *in vivo s*tudies of human islets, islet replacement cells using genetics, small molecules, or modeling of acquired *in vivo* physiological or pathological risk states in diabetes mellitus.

## Methods

### Glucagon gene targeting in NSG mice

*GKO-NSG* mice were generated through the NIDDK Type 1 Diabetes Resource (TIDR) and the Jackson Laboratory. Two mouse *Gcg* Exon 3 guide RNAs (sgRNA 3569: GAAGACAAACGCCACTCACA and sgRNA 3572: CAGACTCTTACCGGTTCCTCT) and

Author Manuscript Author Manuscript Author Manuscript Author Manuscript

the CRISPR/Cas9 plasmid were injected into *NSG (NOD.Cg-Prkdc*$^{scid}$ *Il2rg*$^{tm1Wjl}$*/SzJ*, The Jackson Laboratory, stock 005557) oocytes to generate founders. Out of 33 progeny, one male (termed 18–1) was confirmed by TOPO cloning and DNA sequencing to carry the desired in-frame deletion and bred to *NSG* females for germ line transmission. Verified F1 heterozygous offspring were used for further breeding to homozygosity. Subsequent genotyping were performed using PCR amplification with 3573_F1 (TGAGAACCACTGCAAGGCAAC) and 3575_R1 (AACGATCAATACAGCTAAGGTCTC) primers, which produce a 715 bp wildtype product or a 622 bp *Gcg* exon 3 deletion product (Figure 1b). Homozygous glucagon knockout mice were born at near Mendelian ratios, however some lethality was observed around weaning. To promote survival of *GKO-NSG* mice, mice were provided with DietGel 76A (Clear $H_2O$) mixed with wet chow one week before weaning and for two weeks after weaning. Additionally, mice were provided with water supplemented with 0.045% D-glucose (Sigma-Aldrich) for two weeks after weaning. All mice, including littermate controls, were given this supplemental care. Mice were housed in a pathogen-free barrier facility at Stanford University Medical School, and were exposed to a normal 12-hour light cycle. Male and female mice (2–8 months old) were used for experiments along with age- and sex- matched control littermate *NSG* mice. *GKO-NSG* mice, i.e. NOD.Cg-*Gcg*$^{em1Dvs}$ *Prkdc*$^{scid}$ *Il2rg*$^{tm1Wjl}$/DvsJ (Strain 029819), are available through The Jackson Laboratory.

## Human islet procurement and transplantation

Deidentified human pancreatic islets were procured through the Integrated Islet Distribution Program, Alberta Diabetes Institute IsletCore, and International Institute for the Advancement of Medicine. Five hundred human islet equivalents (IEQ) from previously healthy, nondiabetic organ donors (n=6) or type 2 diabetic donors (n=3) with less than 15-hour cold ischemia time (Table 1) were used for transplantation under the kidney capsule of *GKO-NSG* mice as previously described[8,10]. In brief, 2–5 month-old male and female *GKO-NSG* mice were used as transplantation recipients. Animals were anesthetized using ketamine/xylazine. Upon confirmation of appropriate depth of anesthesia, human islets resuspended in cold Matrigel (Corning) were transferred into the left renal capsular space of recipient mice through a 10ul PCR micro-pipet (Drummond).

## Glucose tolerance testing

After a 5-hour fast (starting from 9–10 AM), mice were administered an intraperitoneal (IP) injection of D-glucose (3 g/kg body weight). Blood glucose levels were measured with a Contour glucometer (Bayer) at 0, 5, 15, 30, 45, 60, 90, and 120 minutes post injection and EDTA-treated plasma samples were collected for insulin hormone assays at the same time intervals. 5–7 month-old male *GKO-NSG, GKO-NSG* Tx, and *NSG* littermate control mice were used. For circulating GLP-1 assessment, mice were fasted for 6 hours (starting at 9AM), then D-glucose (6 g/ kg body weight) was given by oral gavage. Blood glucose was measured with a Contour glucometer (Bayer) at 0, 5, 15, 30, 60, 90, 120, and 180 minutes post-gavage and EDTA-, DPP4-inibitor- (Millipore), and HALT protease inhibitor- (Thermo Scientific) treated plasma samples were collected at 0, 15, and 30 minutes post-gavage. 2.5–3 month-old male and female *GKO-NSG* and *NSG* littermate control mice were used.

Author Manuscript Author Manuscript Author Manuscript Author Manuscript

### Insulin tolerance test (ITT)

After a 5-hour fast (starting from 9–10 AM), mice were administered an intraperitoneal injection of Novolin R U-100 (1U/kg body weight). Blood glucose levels were measured with a Contour glucometer (Bayer) at 0, 15, and 30 minutes post insulin injection. EDTA- and protease cocktail-treated (Bimake) plasma samples were collected at 0 and 30 minutes post-insulin injection for circulating glucagon measurement. 4.5–6.5 month-old male and female *GKO-NSG, GKO-NSG* Tx, *GKO-NSG* Tx T2D, and *NSG* littermate control mice were used.

### Plasma hormones and amino acids assays

Plasma insulin and glucagon levels were assessed using an ultrasensitive mouse insulin ELISA (Mercodia) and glucagon ELISA (Mercodia), respectively. Circulating human insulin levels in transplanted *GKO-NSG* recipients were measured with a human insulin ELISA (Mercodia). Due to ultrasensitive mouse insulin ELISA cross-reactivity with human insulin, mouse insulin from *GKO-NSG* Tx and *GKO-NSG* Tx T2D plasma was determined by subtracting values obtained from human insulin ELISA. 2–7 month-old male and female *GKO-NSG, GKO-NSG* Tx, *GKO-NSG* Tx T2D, and *NSG* littermate control mice were used. Plasma GLP-1 levels were quantified with an active GLP-1 ELISA (Eagle Biosciences) and a total GLP-1 NL-ELISA (Mercodia). 2.5–3 month-old male and female *GKO-NSG, GKO-NSG* Tx, and *NSG* littermate control mice were used. Mice were fasted for 4-hours (starting from 9:30–10:30 AM) prior to blood collection for amino acid quantification. Plasma amino acid levels were determined using a L-Amino Acid Quantitation Kit (Sigma Aldrich) following manufacture's instruction, and individual amino acids by the Vanderbilt University Hormone Assay and Analytical Services Core using a Biochrom 30 amino acid analyzer. 5–7 month-old male and female *GKO-NSG, GKO-NSG* Tx, and *NSG* littermate control mice were used.

### Immunostaining and morphometry

Pancreata were weighed (wet weight), fixed in 4% paraformaldehyde overnight at 4°C, and 10 μm thick cryosections were prepared. At least 10 sections per pancreas spaced at least 100 μm apart were stained with the following primary antibodies: Guinea pig anti-insulin (Dako, 1:500), Rabbit anti-proglucagon (Cell Signaling Technologies, 1:400), Mouse anti-proglucagon (Novus Biologicals, 1:300), Guinea pig anti-glucagon (Takara, 1:2000), Rabbit anti-Mafb (Bethyl, 1:250), Rat anti-Ki67 (Biolegend, 1:100), Rabbit anti-Slc38a5 (Abcam 1:200). Hoechst 33342 (Thermo Fisher Scientific, 1:2000) was used to detect nuclei. For fluorescent detection of primary antibodies, sections were subsequently stained with Alexa Flour-conjugated (488, 555, or 647) secondary antibodies (1:500, donkey-anti-primary-host, Jackson ImmunoResearch). Detailed product information and validation methods are provided in Reporting Summary.

Fluorescent micrographs were captured using a Zeiss AxioM1 microscope and a Leica SP2 confocal microscope. Images were processed in Image J for islet cell mass quantification and Image-Pro Plus for islet cell proliferation using previously described methods[61, 62]. For islet mass analysis, fluorescent micrographs were captured with a 10X objective lens on a Zeiss AxioM1 microscope and individual 10X images were captured as tiled images of

Author Manuscript Author Manuscript Author Manuscript Author Manuscript

entire pancreatic sections using the tiling feature in Zeiss AxioVision software (version 4.8). Pancreata were imaged using fluorescent detectors for secondary antibodies, Hoechst, and an autoflourescent 'background' channel used to capture the entire pancreatic tissue section area. Merged Hoechst and 'background' tiled images were used to measure total pancreatic area, where tissue was manually traced in Image J using the freehand selection tool and areas of traces were measured using the measure function. To measure hormone positive areas, tiled images of individual channels were thresholded and positive areas were measured using the analyze particles function. To calculate islet cell mass, total hormone positive area was divided by the total pancreatic area and then subsequently multiplied by pancreatic weight. For islet proliferation analysis and representative images presented in this manuscript, fluorescent micrographs were captured with a 40x objective lens. 200 islets per pancreata were randomly selected for islet proliferation imaging and analysis. Total α and β cell number were measured using individual channel images and were determined by performing an initial manual count (for each animal) to estimate an average cell number/ fluorescent area; once initial counts were performed, subsequent counting was performed using the automatic bright object count function in Image-Pro Plus software (version 5). Islet cell co-expression of Ki67 and hormones was analyzed using merged channel images; $Ki67^+$ $hormone^+$ cells were manually counted in Image-Pro Plus software (version 5) using the manual count function. 4–8 month-old male and female *GKO-NSG, GKO-NSG* Tx, and *NSG* littermate control mice were used.

## Liver glycogen content assessment

60 mg of tissue from the liver (left lateral lobe) was collected from mice fasted for 5 hours (starting from 9–10 AM), and flash frozen in liquid nitrogen. Liver samples were homogenized on ice in buffer containing protease cocktail inhibitor (Bimake) and quantified using a fluorometric glycogen assay kit according to manufacturer's instructions (Cayman Chemicals). 6–8 month-old male and female *GKO-NSG, GKO-NSG* Tx, and *NSG* littermate control mice were used.

## RNA extraction and quantitative PCR

90 mg of tissue from the liver (left lateral lobe) was collected from mice fasted for 5 hours. Then, total RNA was extracted using RNeasy Mini kit (Qiagen) and complementary DNA was synthesized using Maxima First Strand cDNA Synthesis kit (Thermo Fischer Scientific) following manufacturer's instructions. Quantitative PCR (qPCR) was performed using TaqMan assays (Supplementary Table 1) and reagents from Applied Biosystems with *Actb* used as an endogenous control. 6–8 month-old male *GKO-NSG, GKO-NSG* Tx, and *NSG* littermate control mice were used.

## In vitro glucagon secretion assay

Technical replicates (2–3) containing 25–30 human islets were used for in vitro glucagon secretion assays. Secretion assay media was composed of RPMI 1640 (Gibco) supplemented with 2% fetal bovine serum (HyClone) and the glucose (Sigma-Aldrich) concentrations detailed below. In an initial equilibration step, islets were incubated twice in media containing 7 mM glucose for 45 minutes (90 minutes total). After pre-incubation steps, islets were incubated in media containing 7 mM glucose, 1 mM glucose and, 1 mM glucose + L-

Author Manuscript Author Manuscript Author Manuscript Author Manuscript

Arginine (Sigma-Aldrich) for 60 minutes each and supernatant was collected. At the end of the assay, islets were lysed by sonication in a TE/BSA buffer (10 mM Tris-HCl (Calbiochem), 1 mM EDTA (Calbiochem), and 0.1% BSA (Fisher)) that was subsequently mixed with equal parts of an acid-ethanol solution to extract the total islet glucagon content. Secreted glucagon (from islet supernatant) and total glucagon (islet lysate) were quantified using a glucagon ELISA kit (Mercodia). Measures of secreted glucagon were normalized to total glucagon content (presented as a percentage of total glucagon content). Donor information is listed in Table 1.

## Study approvals

All studies involving human islets were conducted in accordance with Stanford University Institutional Review Board guidelines. All animal experiments and methods were approved by and performed in accordance with the guidelines provided by Institutional Animal Care and Use Committee (IACUC) of Stanford University.

## Statistics

Data are presented as the mean of biological replicates ± SEM with individual data points overlaid. All data are the result of one experiment per biological replicate, where each data point is a distinct biological replicate (n values listed in figure legends), except where noted in Extended Data 5a (figure legend). GraphPad Prism v. 7 and Microsoft Excel 2016 were used to perform Student's t-test (two-tailed), repeated measures ANOVA (with Bonferroni's multiple comparisons test), Mixed-effects analysis (with Bonferroni's multiple comparisons test), and one-way ANOVA (with Tukey's multiple comparisons test) for statistical comparisons between data. For data point values falling below detection limits, statistical tests were run with these data points as 0. As noted in figure legends, data that did not show a normal distribution (plasma glucagon measures from *GKO-NSG* mice) were omitted from statistical tests. $P$ values $\leq 0.05$ were considered significant. Exact $P$ values for data with significant differences are listed in figure legends or in supplementary tables.

Author Manuscript Author Manuscript Author Manuscript Author Manuscript

## Extended Data

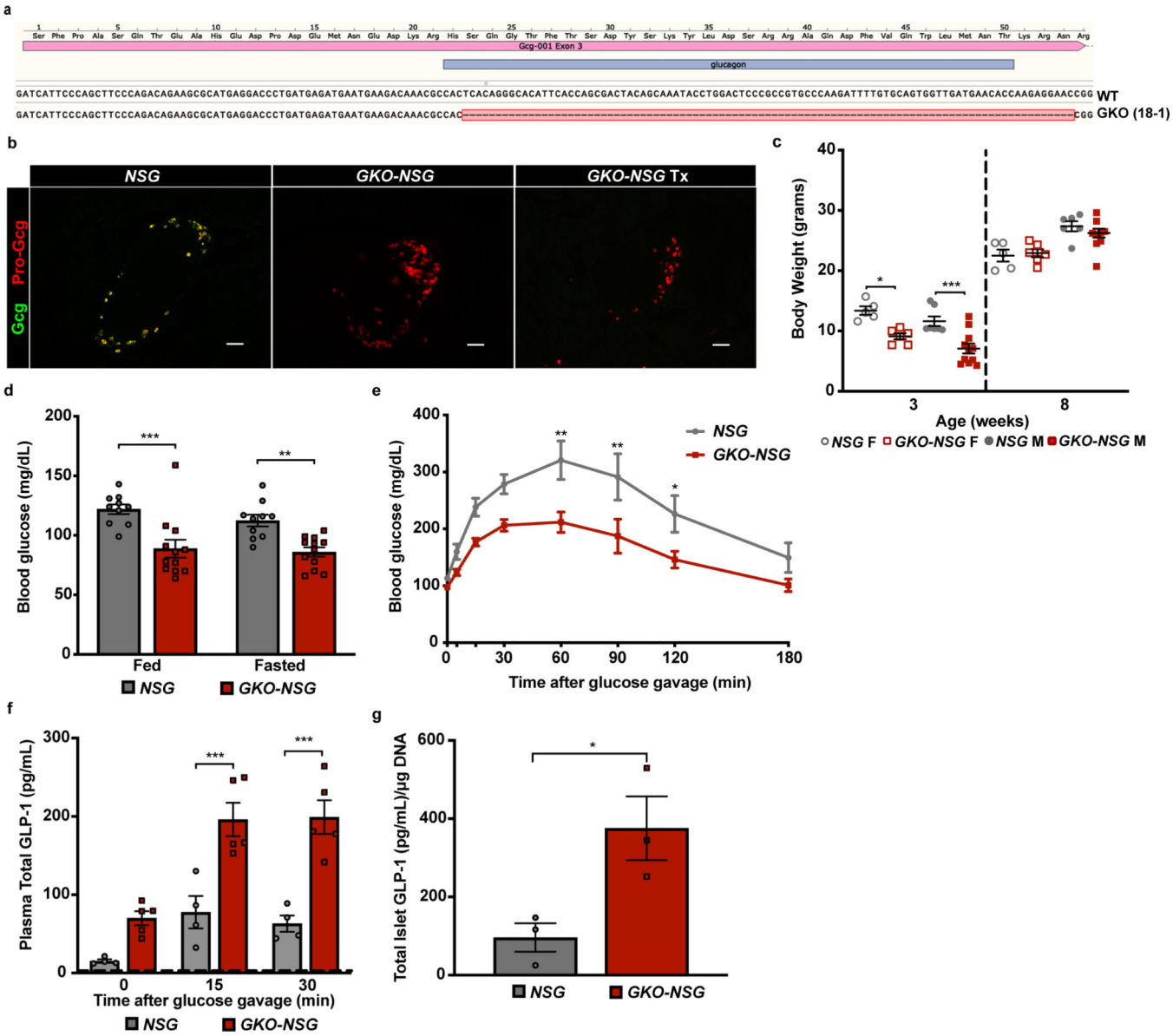


**Extended Data Fig. 1. Design and characterization of *GKO-NSG* mice.**

Related to figure 1. (**a**) Sequence from *GKO-NSG* founder (18–1) showing an in-frame deletion of 93 base pairs within exon 3 of the *Gcg* gene compared to the wild type NSG sequence (WT). Pink bar on top depicts exon 3 of *Gcg*. Blue bar represents nucleotide sequences encoding mature glucagon peptide. Red-highlighted dashes indicate deleted nucleotides in founder 18–1. (**b**) Representative immunostaining of *GKO-NSG* pancreatic islets with antibodies raised against mature glucagon (GCG, green) and proglucagon (Pro-GCG, red) - peptide sequences of GLP-1 (7–17). Similar results were seen across n= 3 *NSG* littermate control, n= 3 *GKO-NSG*, and n= 2 *GKO-NSG* Tx mice. (**c**) Body weight of male and female *GKO-NSG* and *NSG* control littermates at 3 and 8-weeks of age (3-week old female mice $P$= 0.025667 and 3-week old male mice $P$= 0.000454 by Repeated Measures

Author Manuscript Author Manuscript Author Manuscript Author Manuscript

ANOVA, with Tukey's multiple comparisons test) (*NSG* mice, n= 7 males and 5 females; *GKO-NSG* mice, n= 11 males and 6 females). (**d**) Blood glucose measures of 2–3 month old *GKO-NSG* and *NSG* control mice during *ad libitum* feeding or after a 3-hour fast (fed: $P=$ 0.000223; fasted: $P=$ 0.003003 by Repeated Measures ANOVA, with Bonferroni's multiple comparisons test) (*NSG* mice, n= 6 males and 4 females; *GKO-NSG* mice, n= 4 males and 8 females). (**e**) *GKO-NSG* and *NSG* control blood glucose measures over 180 minutes post oral glucose gavage (60': $P=$ 0.001383; 90': $P=$ 0.002618; 120': $P=$ 0.040657 by Repeated Measures ANOVA, with Bonferroni's multiple comparisons test) (6g/kg body weight) (*NSG* mice, n= 5 males and 3 females; *GKO-NSG* mice, n= 8 males and 2 females) and (**f**) plasma total GLP-1 levels from 2.5–3 month old *GKO-NSG* and *NSG* controls following oral glucose challenge (15': $P=$ 0.000194, and 30': $P=$ 0.000034 by Repeated Measures ANOVA, with Bonferroni's multiple comparisons test) (*NSG* mice, n= 4 males; *GKO-NSG* mice, n= 5 males). (**g**) Quantification of active GLP-1 present in islet lysates from 5–7 month old *NSG* (n= 3 males) and *GKO-NSG* (n= 3 males) mice ($P=$ 0.035323 by two-tailed Student's t-test). Dashed lines indicate limit of detection. Scale bars, 50 μm. Data are represented as mean of biological replicates with individual data points overlaid and error bars indicate ± SEM. * $P \leq 0.05$, ** $P \leq 0.01$, *** $P \leq 0.001$.

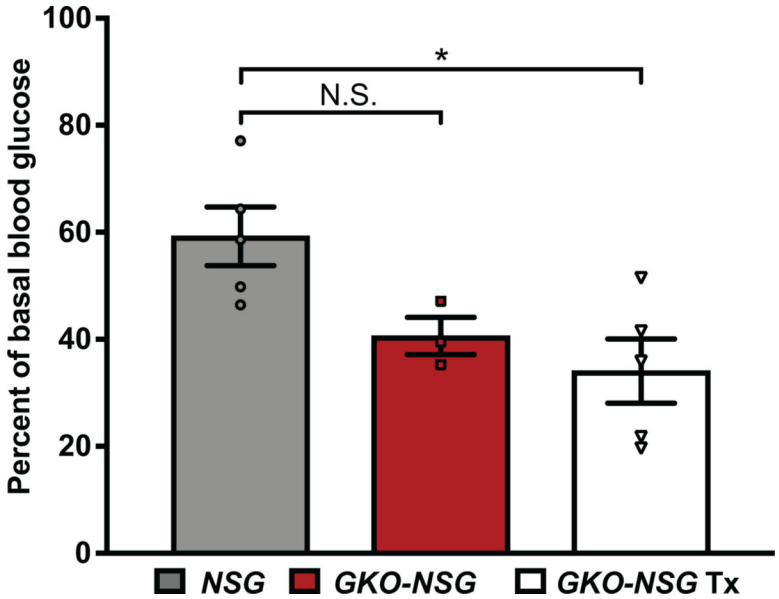


**Extended Data Fig. 2. Blood glucose reduction following insulin challenge.**

Related to Figure 2. Percent of basal blood glucose 30-minutes post insulin injection (1U/kg body weight) from 4.5–6.5 month old *NSG, GKO-NSG, and GKO-NSG Tx* mice (P= 0.017712 by one-way ANOVA, with Tukey's multiple comparison test) (*NSG* mice, n= 5 males; *GKO-NSG* mice, n= 2 males and 1 female; *GKO-NSG* Tx mice, n= 5 males). Data are represented as mean of biological replicates with individual data points overlaid and error bars indicate ± SEM. * $P \leq 0.05$.

Author Manuscript Author Manuscript Author Manuscript Author Manuscript

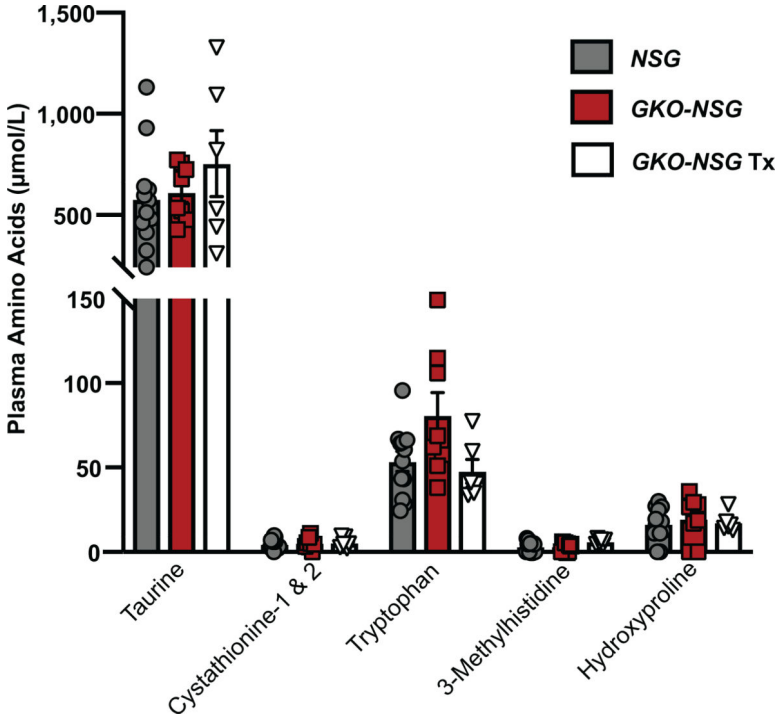


**Extended Data Fig. 3. Concentrations of individual plasma amino acids showing no change in *GKO-NSG* mice.**

Related to Figure 3. Concentration of individual plasma amino acids that showed no significant changes in 6–7 month old *GKO-NSG* mice (*NSG* mice, n= 10 males and 2 females; *GKO-NSG* mice, n= 5 males and 3 females; *GKO-NSG* Tx mice, n= 6 males). Data are represented as mean of biological replicates with individual data points overlaid and error bars indicate ± SEM.

Author Manuscript Author Manuscript Author Manuscript Author Manuscript

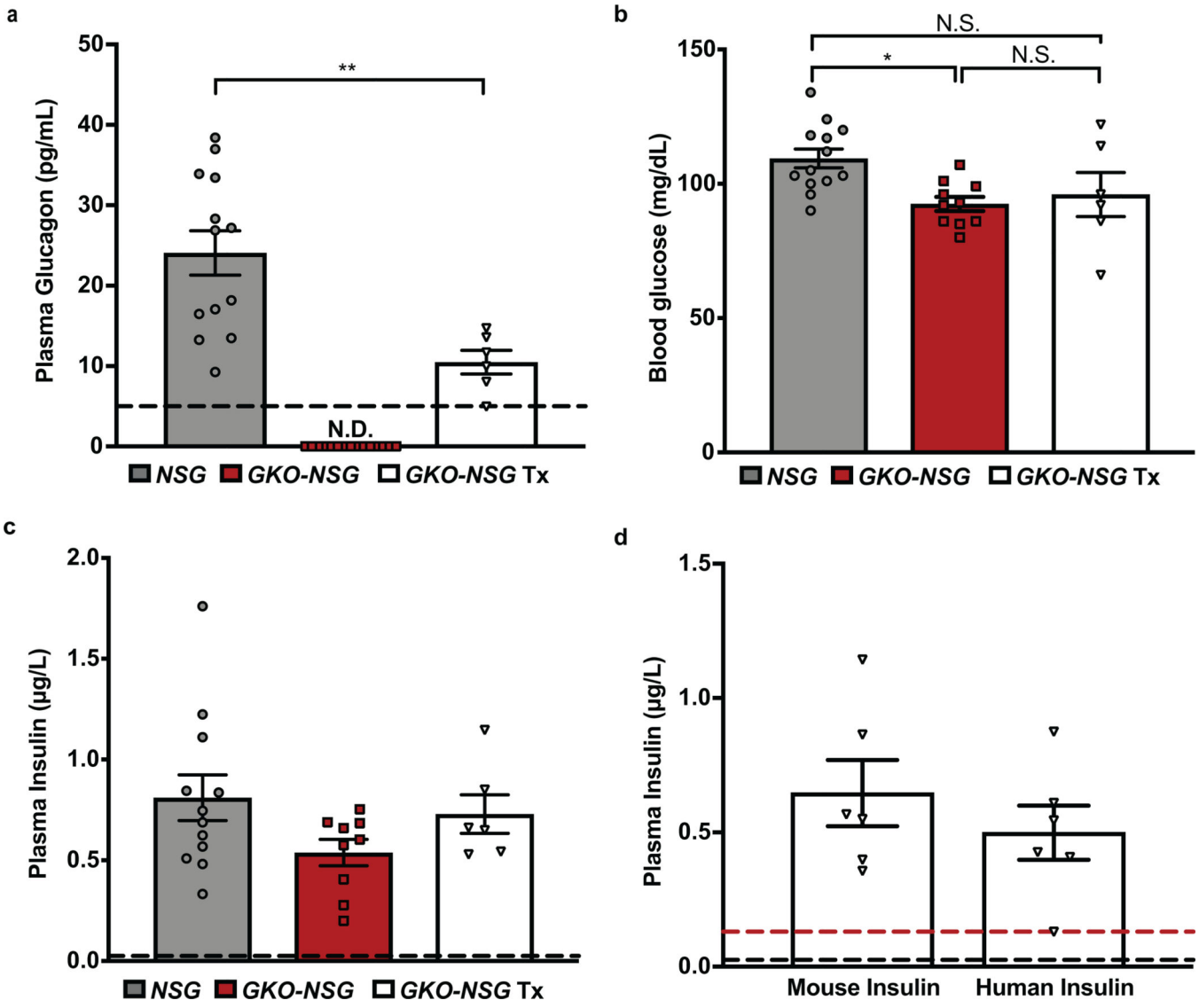


**Extended Data Fig. 4. Further assessment of blood glucose, plasma insulin, and glucagon phenotypes in *GKO-NSG* mice after human islet transplantation.**

Related to Figure 5. Data are from 4–6 month old *NSG* control, *GKO-NSG*, and *GKO-NSG* mice post-transplantation (*GKO-NSG* Tx). (**a**) Plasma glucagon levels in *ad libitum* fed mice (*NSG* vs. *GKO-NSG* Tx: $P$= 0.005112 by two-tailed Student's t-test). Due to the distribution of data from *GKO-NSG* mice, these data points were omitted from statistical analysis. (*NSG* mice, n= 10 males and 3 females; *GKO-NSG* mice, n= 12 males and 1 female; *GKO-NSG* Tx mice, n= 6 males). Blood glucose (**b**) ($P$= 0.013846 by one-way ANOVA, with Tukey's multiple comparison test) (*NSG* mice, n= 10 males and 3 females; *GKO-NSG* mice, n= 8 males and 2 females; *GKO-NSG* Tx mice, n= 6 males) and plasma insulin levels (**c**) (*NSG* mice, n= 10 males and 3 females; *GKO-NSG* mice, n= 7 males and 2 females; *GKO-NSG* Tx mice, n= 6 males) in fasted mice. (**d**) Mouse and human plasma insulin levels in *ad libitum* fed *GKO-NSG Tx* mice (n=6 males). Dashed lines indicate limit of detection (**d**: black dashed line indicates limit of detection of mouse insulin and red

dashed line indicates limit of detection of human insulin). Data are represented as mean of biological replicates with individual data points overlaid and error bars indicate ± SEM. * $P \leq 0.05$, ** $P \leq 0.01$, *** $P \leq 0.001$.

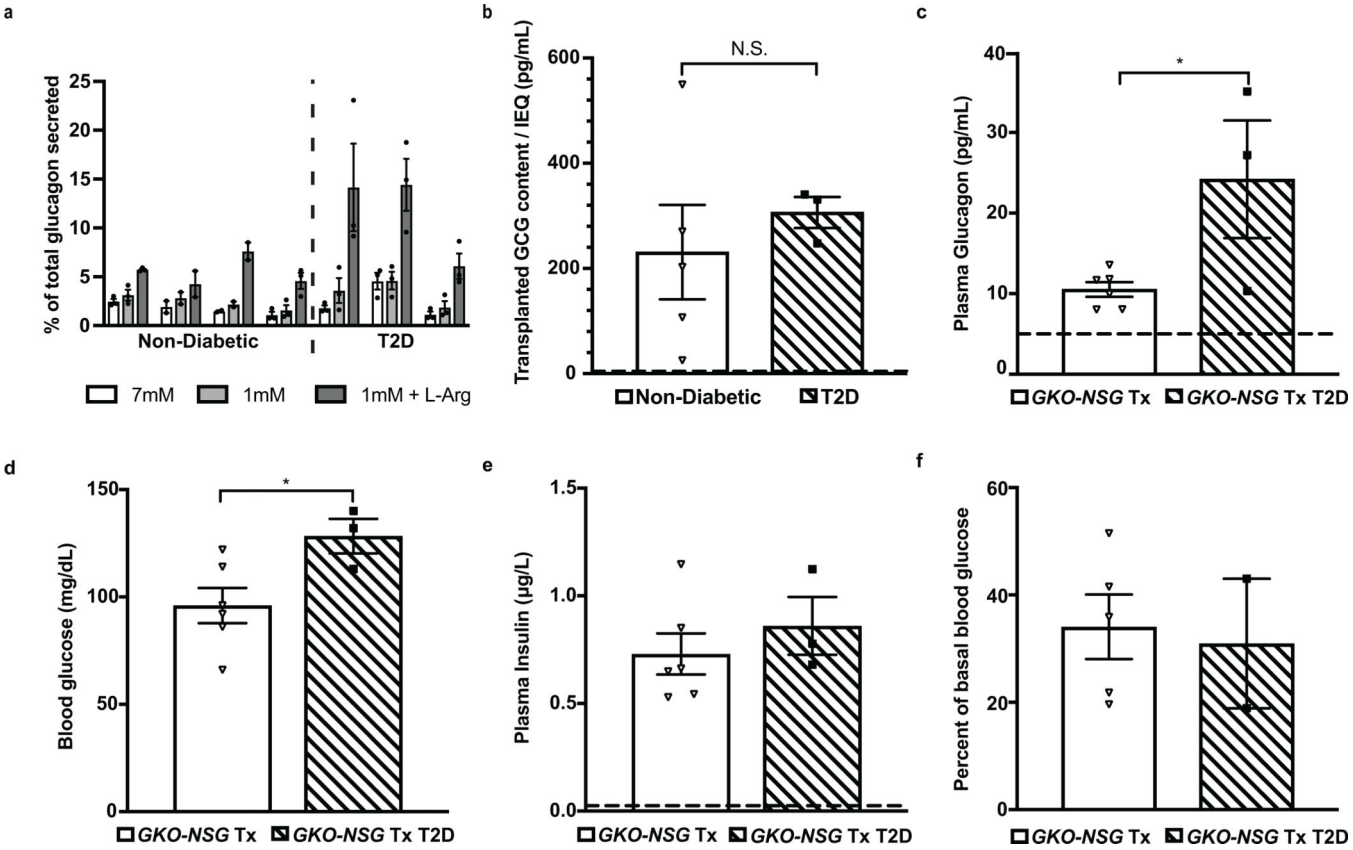


**Extended Data Fig. 5. *In vitro* characterization of donor human islets and more physiological assessment of *GKO-NSG* mice transplanted with islets either non-diabetic or T2D diabetic donors.**

Related to Figure 6. (**a**) *In vitro* glucagon secretion assay on islets from non-diabetic (n= 4 donors) and type 2 diabetic donors (n= 3 donors), shown as technical replicates from individual donors. (**b**) Glucagon content of donor islets transplanted into GKO-NSG mice ($P$=0.558605 by two-tailed Student's t-test; non-diabetic donor n= 5, type 2 diabetic donor n= 3). Data in (**c-e**) are from 4–6 month old *GKO-NSG* mice post-transplantation with islets from non-diabetic (*GKO-NSG* Tx) or type 2 diabetic donors (*GKO-NSG* Tx T2D). For data presented in (**c-e)**: *GKO-NSG* Tx mice, n= 6 males; *GKO-NSG* Tx T2D mice n= 1 male and 2 females. (**c**) Plasma glucagon levels in *ad libitum* fed mice ($P$= 0.034687 by two-tailed Student's t-test). Blood glucose (**d**) ($P$= 0.042886 by two-tailed Student's t-test) and plasma insulin levels (**e**) in 6-hour fasted mice. (**f**) Percent of basal blood glucose 30-minutes post insulin injection (1U/kg body weight) from 4.5–6.5 month old *GKO-NSG Tx* and GKO-NSG Tx T2D mice (*GKO-NSG* Tx mice, n= 5 males; *GKO-NSG* Tx T2D n= 1 male and 1 female). Dashed lines indicate limit of detection. Data are represented as mean of biological replicates with individual data points overlaid, except in **a,** where individual data points



Author Manuscript Author Manuscript Author Manuscript Author Manuscript

Author Manuscript Author Manuscript Author Manuscript Author Manuscript

represent technical replicates from single donors. Error bars indicate ± SEM. * $P \leq 0.05$, ** $P \leq 0.01$, *** $P \leq 0.001$.

## Supplementary Material

Refer to Web version on PubMed Central for supplementary material.

## Acknowledgments

We thank past and current members of the Kim group for advice and encouragement, Dr. S. Park for assistance in gene targeting, Dr. K. Abraham (NIDDK/NIH) for guidance in initial stages of this work, Dr. O. McGuinness and the Vanderbilt University Medical Center Hormone Core (DK059637 and DK020593) for amino acid measurements and advice, Dr. E. Walker for advice on glycogen quantification, the Stanford University Veterinary Service Center for animal care and advice, Dr. C. Sabatti and the Stanford Department of Biomedical Data Science Data Studio for advice on statistical analyses, the Stanford Cell Sciences Imaging Facility for microscope usage, and Dr. D. Serreze (JAX) for generation of mouse lines. We also thank the Integrated Islet Distribution Program (UC4 DK098085-02), Alberta Diabetes Institute IsletCore, and International Institute for the Advancement of Medicine for processing and coordinating human islet distribution. This work was supported by the Type 1 Diabetes Mouse Resource (1UC4DK097610 to D. Serreze), a graduate research fellowship award from the National Science Foundation (DGF-114747 to K. Tellez), RO1 awards (DK107507; DK108817; CA21192701 to S.K.Kim) and a U01 award (DK120447 to Dr. P. MacDonald, Univ. of Alberta). Work in the Stein lab was supported by NIH grants (DK106755, DK050203, and DK090570 to R.W. Stein). Work in the Kim lab was also supported by NIH grant P30 DK116074, the HL Snyder Foundation, the Mulberry Foundation, a gift from S. and M. Kirsch, and by the Stanford Islet Research Core, and Diabetes Genomics and Analysis Core of the Stanford Diabetes Research Center.

## References:

1. Gromada J, Franklin I. & Wollheim CB α-Cells of the Endocrine Pancreas: 35 Years of Research but the Enigma Remains. Endocr. Rev 28, 84–116 (2007). [PubMed: 17261637]
2. McKnight KD, Wang P. & Kim SK Deconstructing pancreas development to reconstruct human islets from pluripotent stem cells. Cell Stem Cell 6, 300–8 (2010). [PubMed: 20362535]
3. Xin Y. et al. RNA Sequencing of Single Human Islet Cells Reveals Type 2 Diabetes Genes. Cell Metab. 24, 608–615 (2016). [PubMed: 27667665]
4. Arda HE et al. Age-Dependent Pancreatic Gene Regulation Reveals Mechanisms Governing Human β Cell Function. Cell Metab. 23, 909–920 (2016). [PubMed: 27133132]
5. Rodriguez-Diaz R. et al. Alpha cells secrete acetylcholine as a non-neuronal paracrine signal priming beta cell function in humans. Nat. Med 17, 888–892 (2011). [PubMed: 21685896]
6. Ishikawa F. et al. Development of functional human blood and immune systems in NOD/SCID/IL2 receptor {gamma} chain(null) mice. Blood 106, 1565–73 (2005). [PubMed: 15920010]
7. Shultz LD et al. Human lymphoid and myeloid cell development in NOD/LtSz-scid IL2R gamma null mice engrafted with mobilized human hemopoietic stem cells. J. Immunol 174, 6477–89 (2005). [PubMed: 15879151]
8. Dai C. et al. Age-dependent human β cell proliferation induced by glucagon-like peptide 1 and calcineurin signaling. J. Clin. Invest 127, 3835–3844 (2017). [PubMed: 28920919]
9. Dai C. et al. Stress-impaired transcription factor expression and insulin secretion in transplanted human islets. J. Clin. Invest 126, 1857–1870 (2016). [PubMed: 27064285]
10. Peiris H. et al. Discovering human diabetes-risk gene function with genetics and physiological assays. Nat. Commun 9, 3855 (2018). [PubMed: 30242153]
11. Bell GI, Sanchez-Pescador R, Laybourn PJ & Najarian RC Exon duplication and divergence in the human preproglucagon gene. Nature 304, 368–371 (1983). [PubMed: 6877358]
12. Heinrich G, Gros P. & Habener JF Glucagon gene sequence. Four of six exons encode separate functional domains of rat pre-proglucagon. J. Biol. Chem 259, 14082–7 (1984). [PubMed: 6094539]

Author Manuscript Author Manuscript Author Manuscript Author Manuscript


13. Drucker DJ, Philippe J, Mojsov S, Chick WL & Habener JF Glucagon-like peptide I stimulates insulin gene expression and increases cyclic AMP levels in a rat islet cell line. Proc. Natl. Acad. Sci. U. S. A 84, 3434–8 (1987). [PubMed: 3033647]
14. Holst JJ The Physiology of Glucagon-like Peptide 1. Physiol. Rev 87, 1409–1439 (2007). [PubMed: 17928588]
15. Cho YM, Fujita Y. & Kieffer TJ Glucagon-Like Peptide-1: Glucose Homeostasis and Beyond. Annu. Rev. Physiol 76, 535–559 (2014). [PubMed: 24245943]
16. Drucker DJ, Habener JF & Holst JJ Discovery, characterization, and clinical development of the glucagon-like peptides. J. Clin. Invest 127, 4217–4227 (2017). [PubMed: 29202475]
17. Knop FK EJE PRIZE 2018: A gut feeling about glucagon. Eur. J. Endocrinol 178, R267–R280 (2018). [PubMed: 29678923]
18. Hayashi Y. et al. Mice Deficient for Glucagon Gene-Derived Peptides Display Normoglycemia and Hyperplasia of Islet α-Cells But Not of Intestinal L-Cells. Mol. Endocrinol 23, 1990–1999 (2009). [PubMed: 19819987]
19. Gelling RW et al. Lower blood glucose, hyperglucagonemia, and pancreatic cell hyperplasia in glucagon receptor knockout mice. Proc. Natl. Acad. Sci 100, 1438–1443 (2003). [PubMed: 12552113]
20. Solloway MJ et al. Glucagon Couples Hepatic Amino Acid Catabolism to mTOR- Dependent Regulation of α-Cell Mass. Cell Rep. 12, 495–510 (2015). [PubMed: 26166562]
21. Dean ED et al. Interrupted Glucagon Signaling Reveals Hepatic α Cell Axis and Role for L-Glutamine in α Cell Proliferation. Cell Metab. 25, 1362–1373.e5 (2017). [PubMed: 28591638]
22. Kim J. et al. Amino Acid Transporter Slc38a5 Controls Glucagon Receptor Inhibition- Induced Pancreatic α Cell Hyperplasia in Mice. Cell Metab. 25, 1348–1361 (2017). [PubMed: 28591637]
23. Furuta M. et al. Defective prohormone processing and altered pancreatic islet morphology in mice lacking active SPC2. Proc. Natl. Acad. Sci. U. S. A 94, 6646–51 (1997). [PubMed: 9192619]
24. Webb GC, Akbar MS, Zhao C, Swift HH & Steiner DF Glucagon replacement via micro-osmotic pump corrects hypoglycemia and alpha-cell hyperplasia in prohormone convertase 2 knockout mice. Diabetes 51, 398–405 (2002). [PubMed: 11812747]
25. Fowden AL The role of insulin in fetal growth. Early Hum. Dev 29, 177–181 (1992). [PubMed: 1396233]
26. Milner RDG & Hill DJ Fetal growth control: the role of insulin and related peptides. Clin. Endocrinol. (oxf). 21, 415–433 (1984). [PubMed: 6096045]
27. Vuguin PM et al. Ablation of the Glucagon Receptor Gene Increases Fetal Lethality and Produces Alterations in Islet Development and Maturation. Endocrinology 147, 3995–4006 (2006). [PubMed: 16627579]
28. Ouhilal S. et al. Hypoglycemia, hyperglucagonemia, and fetoplacental defects in glucagon receptor knockout mice: a role for glucagon action in pregnancy maintenance. Am. J. Physiol. Metab 302, E522–E531 (2012).
29. Cheng X. et al. Glucagon contributes to liver zonation. Proc. Natl. Acad. Sci. U. S. A 115, E4111–E4119 (2018). [PubMed: 29555772]
30. Ohneda A, Aguilar-Parada E, Eisentraut AM & Unger RH Control of pancreatic glucagon secretion by glucose. Diabetes 18, 1–10 (1969). [PubMed: 5761864]
31. Miller RA et al. Targeting hepatic glutaminase activity to ameliorate hyperglycemia. Nat. Med 24, 518–524 (2018). [PubMed: 29578539]
32. Holst JJ, Wewer Albrechtsen NJ, Pedersen J. & Knop FK Glucagon and Amino Acids Are Linked in a Mutual Feedback Cycle: The Liver-α-Cell Axis. Diabetes 66, 235–240 (2017). [PubMed: 28108603]
33. Hancock AS, Du A, Liu J, Miller M. & May CL Glucagon Deficiency Reduces Hepatic Glucose Production and Improves Glucose Tolerance In Adult Mice. Mol. Endocrinol 24, 1605–1614 (2010). [PubMed: 20592160]
34. Vincent M. et al. Abrogation of Protein Convertase 2 Activity Results in Delayed Islet Cell Differentiation and Maturation, Increased α-Cell Proliferation, and Islet Neogenesis. Endocrinology 144, 4061–4069 (2003). [PubMed: 12933680]

Author Manuscript Author Manuscript Author Manuscript Author Manuscript

35. Artner I. et al. MafB: an activator of the glucagon gene expressed in developing islet alpha- and beta-cells. Diabetes 55, 297–304 (2006). [PubMed: 16443760]
36. Schaum N. et al. Single-cell transcriptomics of 20 mouse organs creates a Tabula Muris. Nature 562, 367–372 (2018). [PubMed: 30283141]
37. Sørensen H. et al. Immunoneutralization of endogenous glucagon reduces hepatic glucose output and improves long-term glycemic control in diabetic ob/ob mice. Diabetes 55, 2843–8 (2006). [PubMed: 17003351]
38. Svendsen B. et al. Insulin Secretion Depends on Intra-islet Glucagon Signaling. Cell Reports 25, 1127–1134.e2 (2018). [PubMed: 30380405]
39. Capozzi ME et al. Glucagon lowers glycemia when β-cells are active. JCI Insight (2019). doi:10.1172/JCI.INSIGHT.129954
40. Müller WA, Faloona GR, Aguilar-Parada E. & Unger RH Abnormal Alpha-Cell Function in Diabetes. N. Engl. J. Med 283, 109–115 (1970). [PubMed: 4912452]
41. Reaven GM, Chen Y-DI, Golay A, Swislocki ALM & Jaspan JB Documentation of Hyperglucagonemia Throughout the Day in Nonobese and Obese Patients with Noninsulin-Dependent Diabetes Mellitus*. J. Clin. Endocrinol. Metab 64, 106–110 (1987). [PubMed: 3536980]
42. Bozadjieva N. et al. Loss of mTORC1 signaling alters pancreatic α cell mass and impairs glucagon secretion. J. Clin. Invest 127, 4379–4393 (2017). [PubMed: 29106387]
43. Müller TD, Finan B, Clemmensen C, DiMarchi RD & Tschöp MH The New Biology and Pharmacology of Glucagon. Physiol. Rev 97, 721–766 (2017). [PubMed: 28275047]
44. Rodriguez-Diaz R. et al. Paracrine Interactions within the Pancreatic Islet Determine the Glycemic Set Point. Cell Metab. 27, 549–558.e4 (2018). [PubMed: 29514065]
45. Schwartz NS, Clutter WE, Shah SD & Cryer PE Glycemic thresholds for activation of glucose counterregulatory systems are higher than the threshold for symptoms. J. Clin. Invest 79, 777–81 (1987). [PubMed: 3546378]
46. Arda HE et al. A Chromatin Basis for Cell Lineage and Disease Risk in the Human Pancreas. Cell Syst. 7, 310–322.e4 (2018). [PubMed: 30145115]
47. Brissova M. et al. α Cell Function and Gene Expression Are Compromised in Type 1 Diabetes. Cell Rep. 22, 2667–2676 (2018). [PubMed: 29514095]
48. Camunas-Soler J. et al. Pancreas patch-seq links physiologic dysfunction in diabetes to single-cell transcriptomic phenotypes. bioRxiv 555110 (2019). doi:10.1101/555110
49. van der Meulen T. et al. Urocortin3 mediates somatostatin-dependent negative feedback control of insulin secretion. Nat. Med 21, 769–776 (2015). [PubMed: 26076035]
50. Arrojo e Drigo R. et al. Structural basis for delta cell paracrine regulation in pancreatic islets. Nat. Commun 10, 3700 (2019). [PubMed: 31420552]
51. Vergari E. et al. Insulin inhibits glucagon release by SGLT2-induced stimulation of somatostatin secretion. Nat. Commun 10, 139 (2019). [PubMed: 30635569]
52. Cejvan K, Coy DH & Efendic S. Intra-islet somatostatin regulates glucagon release via type 2 somatostatin receptors in rats. Diabetes 52, 1176–81 (2003). [PubMed: 12716749]
53. Hauge-Evans AC et al. Somatostatin Secreted by Islet δ-Cells Fulfills Multiple Roles as a Paracrine Regulator of Islet Function. Diabetes 58, 403–411 (2009). [PubMed: 18984743]
54. Patton GS et al. Pancreatic immunoreactive somatostatin release. Proc. Natl. Acad. Sci 74, 2140–2143 (1977). [PubMed: 325567]
55. Weir GC, Samols E, Day JA & Patel YC Glucose and glucagon stimulate the secretion of somatostatin from the perfused canine pancreas. Metabolism 27, 1223–1226 (1978). [PubMed: 682984]
56. Kroon E. et al. Pancreatic endoderm derived from human embryonic stem cells generates glucose-responsive insulin-secreting cells in vivo. Nat Biotechnol 26, 443–452 (2008). [PubMed: 18288110]
57. Micallef SJ et al. INS GFP/w human embryonic stem cells facilitate isolation of in vitro derived insulin-producing cells. Diabetologia 55, 694–706 (2012). [PubMed: 22120512]

Author Manuscript Author Manuscript Author Manuscript Author Manuscript

58. Basford CL et al. The functional and molecular characterisation of human embryonic stem cell-derived insulin-positive cells compared with adult pancreatic beta cells. Diabetologia 55, 358–371 (2012). [PubMed: 22075915]

59. Pagliuca FW et al. Generation of Functional Human Pancreatic β Cells In Vitro. Cell 159, 428–439 (2014). [PubMed: 25303535]

60. Nair GG et al. Recapitulating endocrine cell clustering in culture promotes maturation of human stem-cell-derived β cells. Nat. Cell Biol 21, 263–274 (2019). [PubMed: 30710150]

## Method-only References

61. Chakravarthy H. et al. Converting adult pancreatic islet α cells into β cells by targeting both Dnmt1 and Arx. Cell Metab 25, 622–634. (2017). [PubMed: 28215845]

62. Pauerstein PT et al. A radial axis defined by semaphorin-to-neuropilin signaling controls pancreatic islet morphogenesis. Development 144, 3744–3754. (2017). [PubMed: 28893946]

Author Manuscript Author Manuscript Author Manuscript Author Manuscript

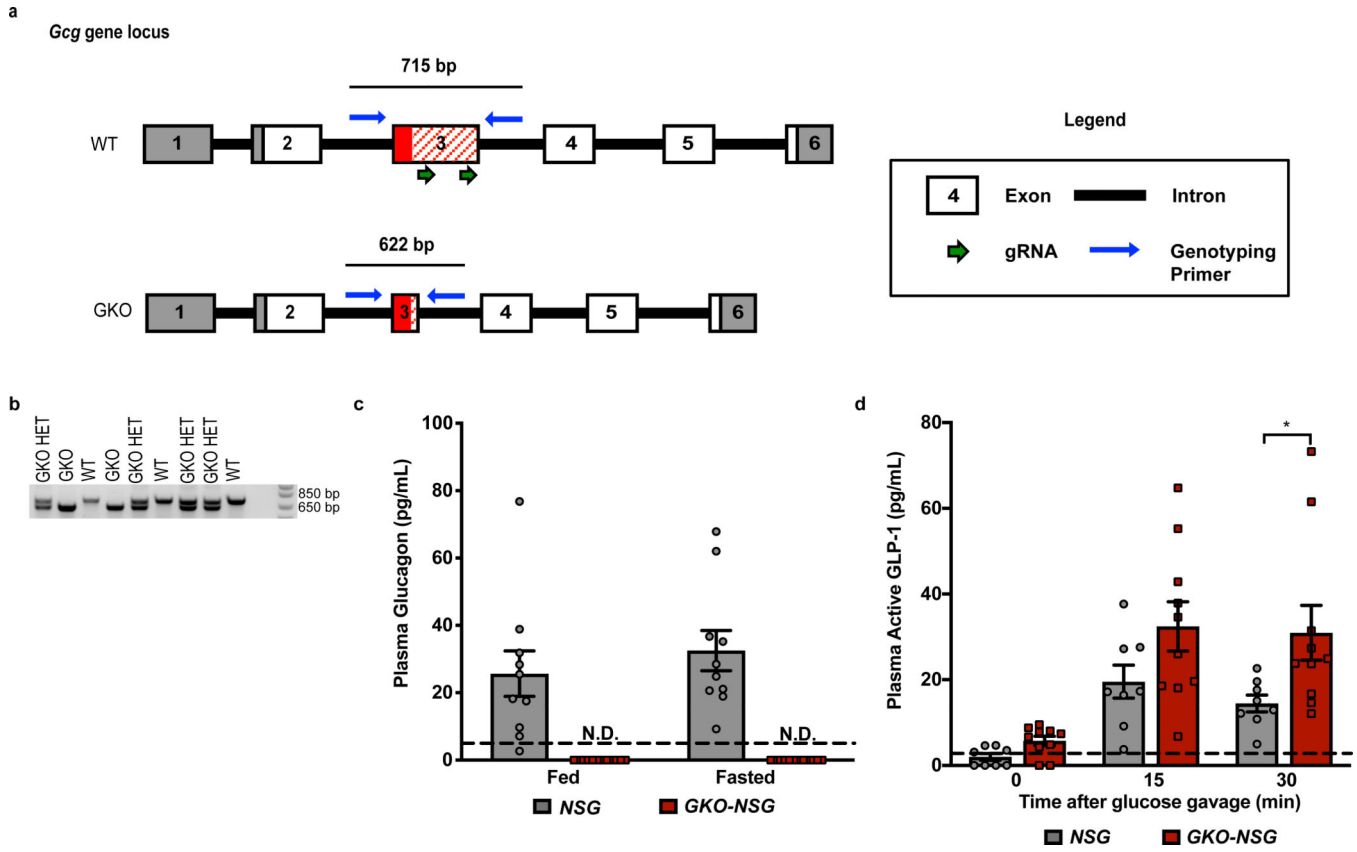


**Figure 1. Generation of *GKO-NSG* mice.**

(**a**) Schematic showing *Glucagon* (*Gcg*) gene structure, guide RNA (gRNA) targeting sites (green arrows), and genotyping primers (blue arrows). Exon 3 is highlighted in red with the portion encoding mature glucagon marked by hatch lines. (**b**) Representative genotyping PCR of *GKO-NSG* mice following a heterozygous *GKO-NSG* cross; similar results were seen from 30 crosses of heterozygous *GKO-NSG* mice. DNA ladder on right side of genotyping gel image is marked at the size indicators for 850 and 650 base pairs (bp). (**c**) Plasma glucagon levels in 2–3 month old *GKO-NSG* and *NSG* mice during *ad libitum* feeding or after a 3-hour fast. Due to distribution of data from *GKO-NSG* mice, these data were not analyzed with statistical tests. (*NSG* mice, n= 6 males and 4 females; *GKO-NSG* mice, n= 4 males and 8 females). (**d**) Plasma active GLP-1 levels from 2.5–3 month old *GKO-NSG* and *NSG* controls following oral glucose challenge (30’: $P$= 0.027573 by Repeated Measures ANOVA, with Bonferroni’s multiple comparisons test) (*NSG* mice, n= 5 males and 3 females; *GKO-NSG* mice, n= 8 males and 2 females). Dashed lines indicate limit of detection. Data are represented as mean of biological replicates with individual data points overlaid and error bars indicate ± SEM. * $P \leq 0.05$, ** $P \leq 0.01$, *** $P \leq 0.001$. N.D.= not detected. See also Extended Data 1.

Author Manuscript Author Manuscript Author Manuscript Author Manuscript

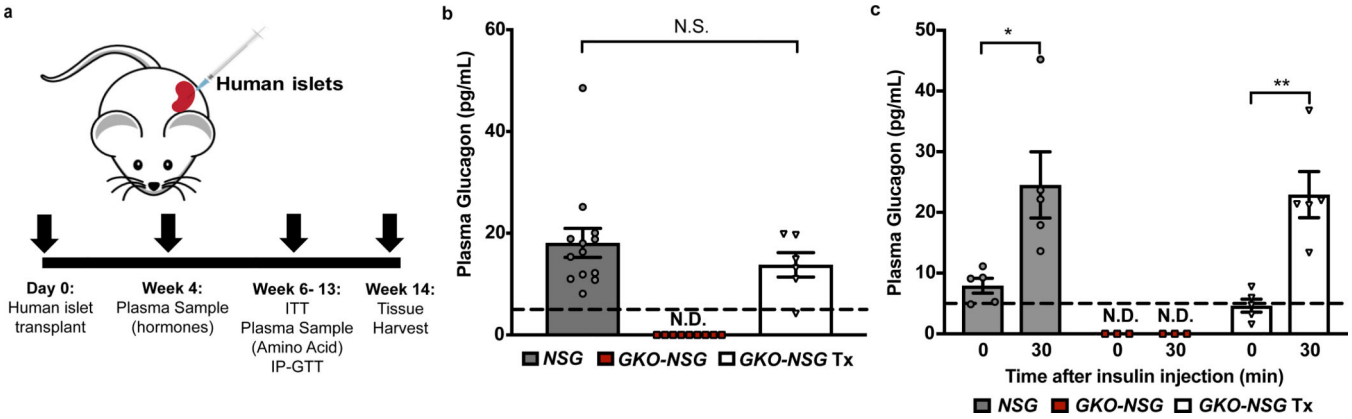


**Figure 2. Transplanted human islets retain regulated glucagon secretion in *GKO-NSG* mice.**

Human islets were transplanted under the renal capsule of *GKO-NSG* mice. Mice were then examined for presence of glucagon in the circulation and regulation of glucagon secretion from transplanted islets. Data are from *NSG* control, *GKO-NSG*, and *GKO-NSG* mice post-transplantation (*GKO-NSG* Tx). (**a**) Schematic of islet transplantation and phenotyping schedule. (**b**) Plasma glucagon levels from 4–6 month old mice after a 6-hour fast. Due to the distribution of data from *GKO-NSG* mice, these data points were omitted from one-way ANOVA, with Tukey's multiple comparisons test. (*NSG* mice, n= 10 males and 3 females; *GKO-NSG* mice, n= 11 males and 2 females; *GKO-NSG* Tx mice, n= 6 males). (**c**) 4.5–6.5 month old mice were challenged with human insulin; glucagon response to acute hypoglycemia was measured from plasma at 0 and 30-minutes post-insulin injection (0' vs 30': *NSG: P*= 0.033030; *GKO-NSG* Tx: *P*= 0.002262 by paired two-tailed Student's t-test, with Bonferroni correction). Due to the distribution of data from *GKO-NSG* mice, these data points were omitted from statistical analysis. (*NSG* mice, n= 5 males; *GKO-NSG* mice, n= 2 males and 1 female; *GKO-NSG* Tx mice, n= 5 males). Dashed lines indicate limit of detection. Data are represented as mean of biological replicates with individual data points overlaid and error bars indicate ± SEM. N.D.= not detected. N.S.= not significant. * $P \leq 0.05$, ** $P \leq 0.01$, *** $P \leq 0.001$. See also Extended Data 2.

Author Manuscript Author Manuscript Author Manuscript Author Manuscript

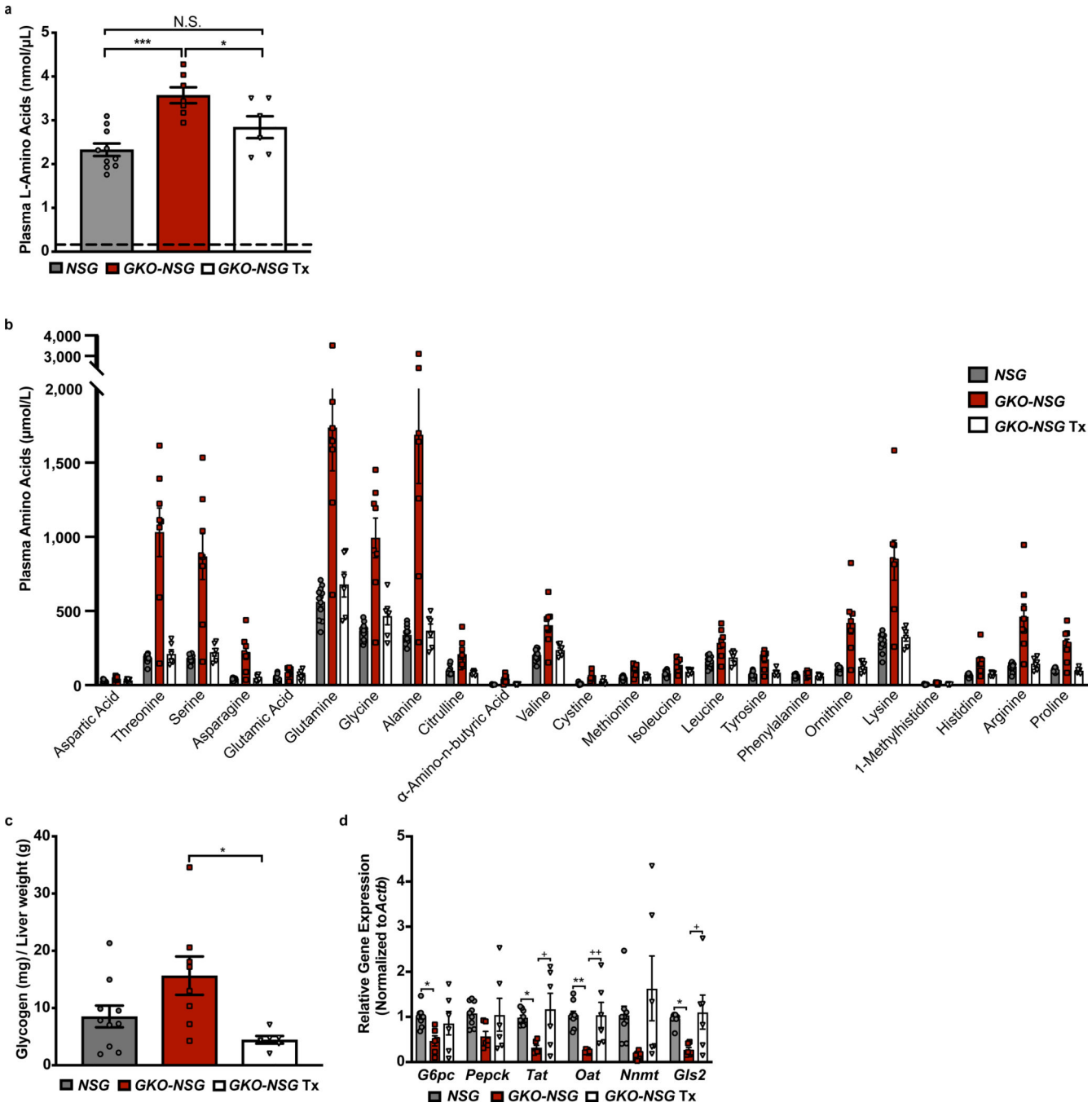


**Figure 3. Human islet transplantation establishes a glucagon-signaling axis that corrects liver phenotypes in *GKO-NSG* mice.**

Mice were examined for liver phenotypes associated with glucagon loss following transplantation of human islets. Data are from *NSG* control, *GKO-NSG*, and *GKO-NSG* mice post-transplantation (*GKO-NSG* Tx). (**a**) Total plasma amino acids from 5–7 month old mice (*NSG* vs. *GKO-NSG* $P$= 0.000198; *GKO-NSG* vs. *GKO-NSG* Tx $P$= 0.044206 by one-way ANOVA, with Tukey's multiple comparisons test) (*NSG* mice, n= 8 males and 2 females; *GKO-NSG* mice, n= 4 males and 3 females; *GKO-NSG* Tx mice, n= 6 males). (**b**)

Author Manuscript Author Manuscript Author Manuscript Author Manuscript

Concentration of individual plasma amino acids that showed significant change in *GKO-NSG* mice by one-way ANOVA, with Tukey's multiple comparisons test (*P* values listed in Supplementary Table 2) (*NSG* mice, n= 10 males and 2 females; *GKO-NSG* mice, n= 5 males and 3 females; *GKO-NSG* Tx mice, n= 6 males). (**c**) Liver glycogen quantification from the left lobe of 6–8 month old mice (*GKO-NSG* vs. *GKO-NSG* Tx: $P$= 0.015738 by one-way ANOVA, with Tukey's multiple comparisons test) (*NSG* mice, n= 9 males and 1 female; *GKO-NSG* mice, n= 6 males and 2 females; *GKO-NSG* Tx mice, n= 6 males). (**d**) Gene expression in the left liver lobe of indicated genes from 6–8 month old mice (significant *P* values generated by one-way ANOVA, with Tukey's multiple comparisons test are listed in Supplementary Table 2) (*NSG* mice, n= 9 males; *GKO-NSG* mice, n= 6 males; *GKO-NSG* Tx mice, n= 6 males). Dashed lines indicate limit of detection. Data are represented as mean of biological replicates with individual data points overlaid and error bars indicate ± SEM. N.S.= not significant. * *NSG* vs. *GKO-NSG* mice and $^{+}$ *GKO-NSG* vs. *GKO-NSG Tx* mice (**b** and **d**). $^{+}$ or * $P \leq 0.05$, $^{++}$or ** $P \leq 0.01$, $^{+++}$ or *** $P \leq 0.001$. See also Supplementary Table 2 and Extended Data 3.

Author Manuscript Author Manuscript Author Manuscript Author Manuscript

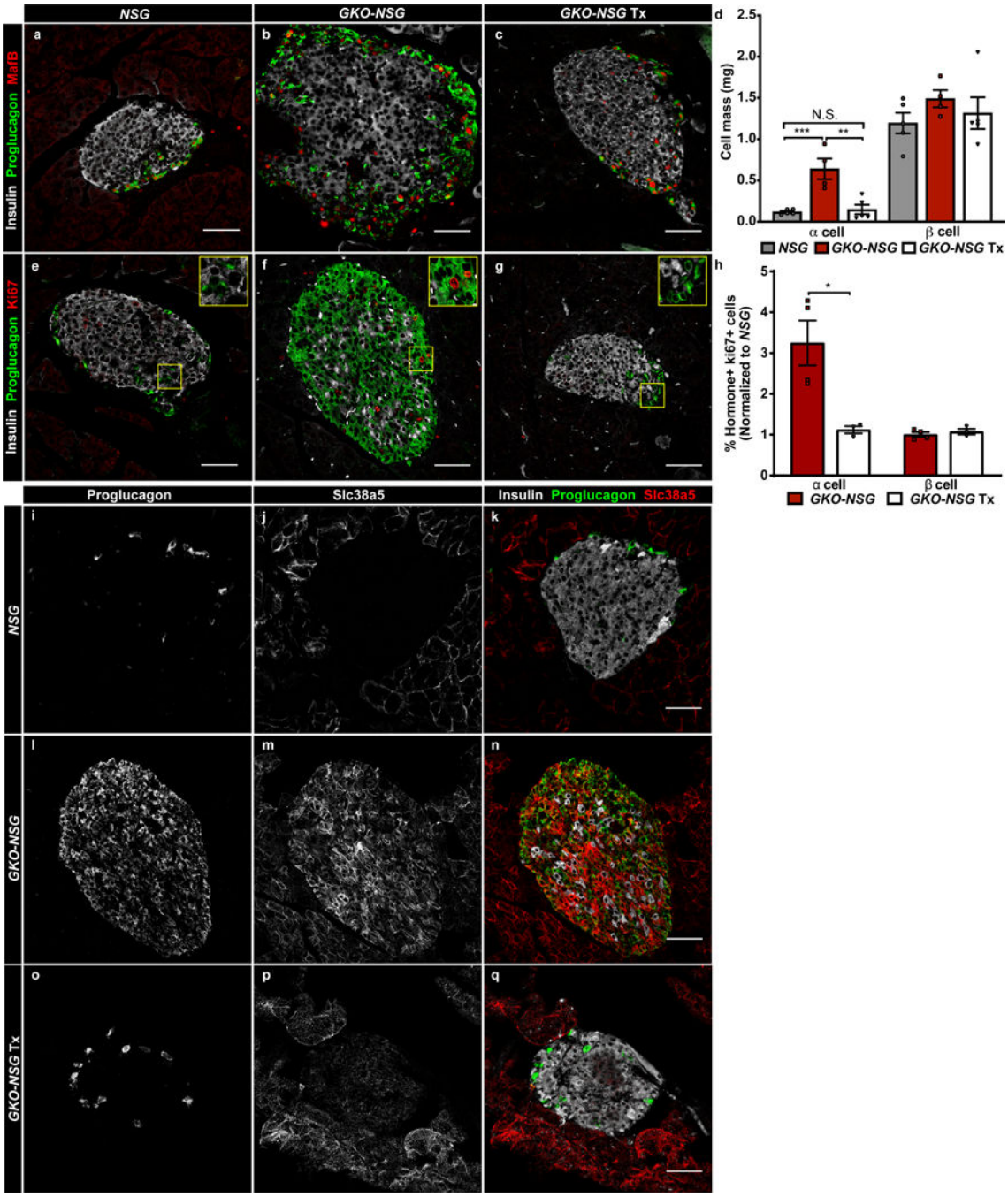


**Figure 4. Human islet-derived glucagon corrects *GKO-NSG* α cell hyperplasia.**

(**a-c**) Representative immunostaining for quantification of α and β cell mass (**d**) from 4–8 month old *NSG* control, *GKO-NSG*, and *GKO-NSG* Tx mice with antibodies detecting Proglucagon (green), Insulin (white), and MafB (red) (*NSG* vs. *GKO-NSG* $P$= 0.000958; *GKO-NSG* vs. *GKO-NSG* Tx $P$= 0.001530 by one-way ANOVA, with Tukey's multiple comparisons test) (*NSG* mice, n= 3 males and 1 female; *GKO-NSG* mice, n= 3 males and 1 female; *GKO-NSG* Tx mice, n= 5 males). (**e-g**) Representative immunostaining for quantification of α and β cell proliferation (**h**) in 4–8 month old *NSG* control, *GKO-NSG*,

Author Manuscript Author Manuscript Author Manuscript Author Manuscript

and *GKO-NSG* Tx mouse pancreata using antibodies detecting Proglucagon (green), Insulin (white), and Ki67 (red). ($P$= 0.022675 by two-tailed Student's t-test) (*NSG* mice, n= 3 males and 1 female; *GKO-NSG* mice, n= 3 males and n= 1 female; *GKO-NSG* Tx mice, n= 3 males). For (**a-h**): images for morphometric quantifications are acquired from 10 pancreatic sections per individual mouse (see methods). (**i-q**) Representative immunostaining of Slc38a5 expression in *NSG* control, *GKO-NSG*, and *GKO-NSG* Tx mouse pancreata using antibodies detecting Proglucagon (green), Insulin (white), and Slc38a5 (red). Similar results for Slc38a5 staining were seen across n= 3 *NSG* control, n= 5 *GKO-NSG*, and n= 3 *GKO-NSG* Tx mice. All images are shown at the same resolution; scale bars, 50 **μ**m. Data are represented as mean of biological replicates with individual data points overlaid and error bars indicate ± SEM. N.S.= not significant. * $P \leq 0.05$, ** $P \leq 0.01$, *** $P \leq 0.001$.

Author Manuscript Author Manuscript Author Manuscript Author Manuscript

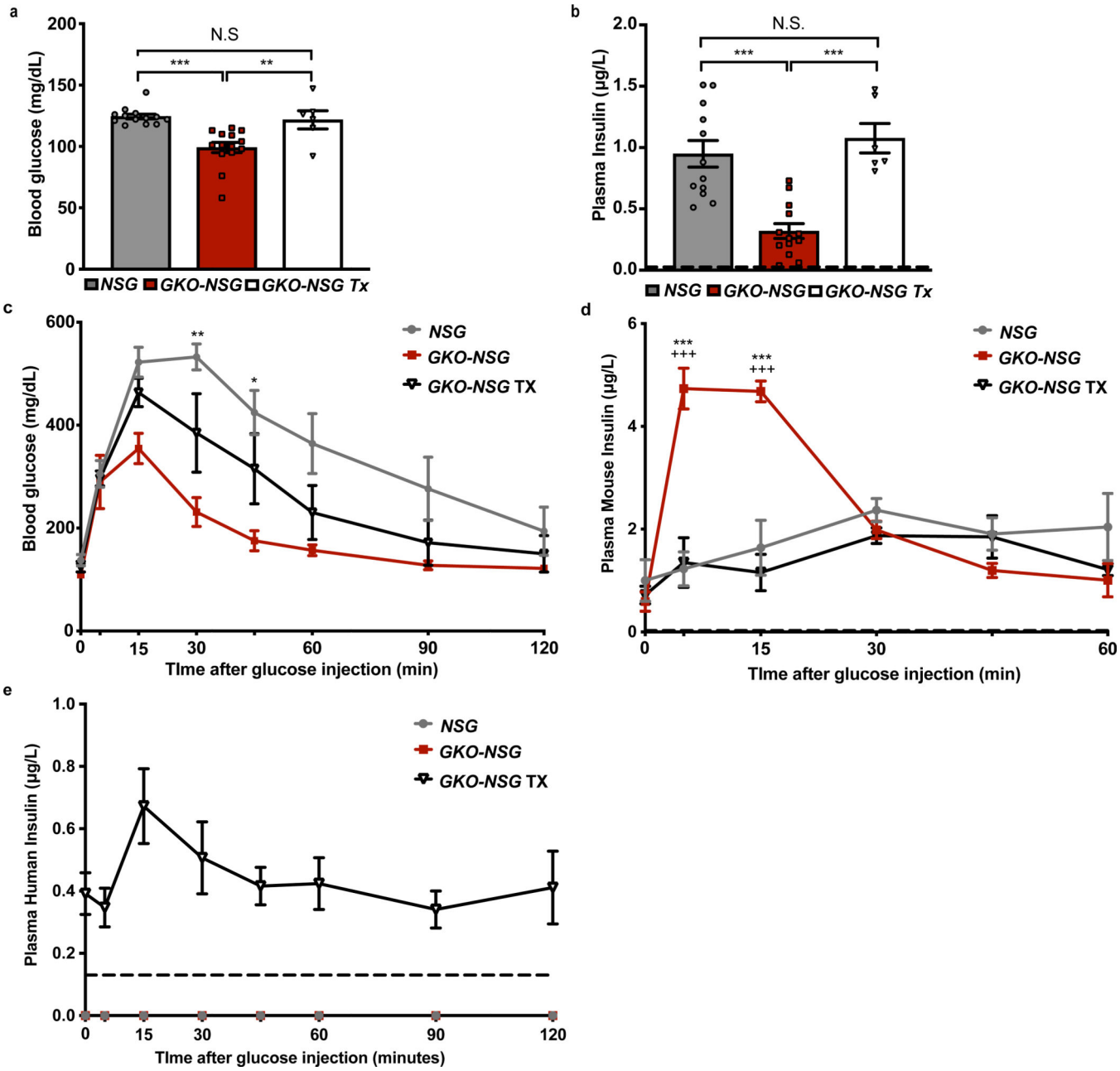


**Figure 5. Improved glucose and insulin regulation in transplanted *GKO-NSG* mice.**

4–6 month old *GKO-NSG* mice post-transplantation (*GKO-NSG* Tx), *GKO-NSG* mice, and *NSG* control mice were assessed for *ad libitum* fed blood glucose (**a**) (*NSG* vs. *GKO-NSG* $P$= 0.000086; *GKO-NSG* vs. *GKO-NSG* Tx $P$= 0.004522 by one-way ANOVA, with Tukey's multiple comparisons test) (*NSG* mice, n= 10 males and 3 females; *GKO-NSG* mice, n= 12 males and 2 females; *GKO-NSG* Tx mice, n= 6 males) and plasma insulin levels (**b**) (*NSG* vs. *GKO-NSG* $P$= 0.000047; *GKO-NSG* vs. *GKO-NSG* Tx $P$= 0.000066 by one-way ANOVA with Tukey's multiple comparisons test) (*NSG* mice, n= 9 males and 3 females; *GKO-NSG* mice, n= 11 males and 2 females; *GKO-NSG* Tx mice, n= 6 males). 5–7 month old mice were given an intraperitoneal glucose tolerance test and monitored for

Author Manuscript Author Manuscript Author Manuscript Author Manuscript

blood glucose measures (**c**) and plasma mouse (**d**) and human (**e**) insulin levels (*P* values generated by Repeated Measures ANOVA, with Tukey's multiple comparisons test are listed in Supplementary Table 3). For (**c-e**): *NSG* mice, n= 3 males; *GKO-NSG* mice, n= 3 males; *GKO-NSG* Tx mice, n= 4 males. Human insulin excursion is measured by human insulin-specific ELISA in the same IPGTT test as in panels (**c**) and (**d**). Dashed lines indicate limit of detection. Data are represented as mean of biological replicates with individual data points overlaid and error bars indicate ± SEM. N.S.= not significant. * *NSG* vs. *GKO-NSG* mice and $^{+}$ *GKO-NSG* vs. *GKO-NSG* Tx mice (**c-d**). $^{+}$ or * $P \leq 0.05$, $^{++}$ or ** $P \leq 0.01$, $^{+++}$ or *** $P \leq 0.001$. See also Supplementary Table 3 and Extended Data 4.

Author Manuscript Author Manuscript Author Manuscript Author Manuscript

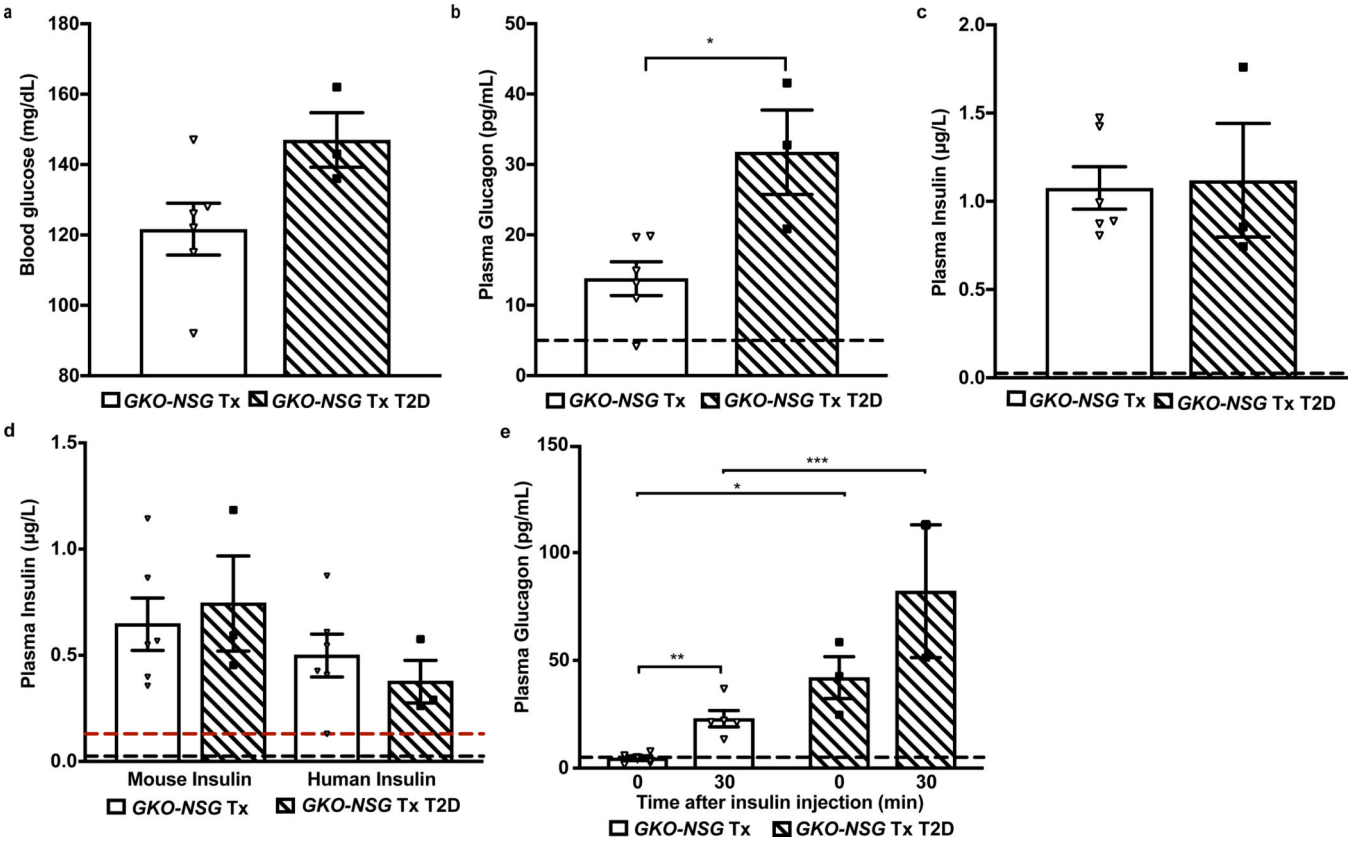


**Figure 6. Excessive glucagon secretion by transplanted T2D islets in *GKO-NSG* mice.**

4–6 month old *GKO-NSG* mice transplanted with islets from non-diabetic (*GKO-NSG* Tx) or T2D diabetic (*GKO-NSG* Tx T2D) donors were assessed for *ad libitum* fed blood glucose levels (**a**), 6-hour fasted plasma glucagon levels (**b**) ($P$= 0.015626 by two-tailed Student's t-test), and *ad libitum* fed plasma insulin levels (**d**). In (**d**), black dashed line indicates limit of detection for mouse insulin and red dashed line indicates limit of detection for human insulin. (**e**) 4.5–6.5 month old mice were challenged with human insulin; glucagon response to acute hypoglycemia was measured from plasma at 0 and 30-minutes post-insulin injection (0' vs 30': *GKO-NSG* Tx $P$= 0.002262 by paired two-tailed t-test, with Bonferroni correction) (*GKO-NSG* Tx vs. *GKO-NSG* Tx T2D 0': $P$= 0.013266; 30': $P$= 0.000985 by Mixed-effects analysis, with Bonferroni's multiple comparisons test). For all data in (**a-e**), *GKO-NSG* Tx mice, n= 6 males; *GKO-NSG* Tx T2D n= 1 male and 2 females. Dashed lines indicate limit of detection. Data are represented as mean of biological replicates with individual data points overlaid and error bars indicate ± SEM. * $P \leq 0.05$, ** $P \leq 0.01$, *** $P \leq 0.001$. See also Extended Data 5.

Author Manuscript Author Manuscript Author Manuscript Author Manuscript

**Table 1.**

Donor information of human islets used for transplantation studies

| Sample ID | Source ID | Age | Sex | BMI | Purity | HbA1c |
|---|---|---|---|---|---|---|
| 1 | SAMN08773444 | 40 | M | 25.5 | 95% | 5.3 |
| 2 | R278 | 57 | M | 27.6 | 80% | 5.7 |
| 3 | SAMN09862214 | 31 | M | 31.8 | 80% | 5.3 |
| 4 | R292 | 47 | M | 27.6 | 90% | 5.6 |
| 5 | SAMN10574375 | 60 | F | 30.6 | 80% | 6 |
| 6 | R338 | 30 | M | 25.5 | 90% | 5.3 |
| 7 | SAMN11157311 | 34 | F | 31.7 | 92% | 7.3 |
| 8 | AGJU173 | 53 | F | 29.2 | 75% | 9.8 |
| 9 | R347 | 57 | M | 27.9 | 75% | 6.3 |